Medicinal Chemistry Research (2021) 30:1868–1885
https://doi.org/10.1007/s00044-021-02773-y

MEDICINAL CHEMISTRY RESEARCH

ORIGINAL RESEARCH

Synthesis and antiproliferative activity of hybrid thiosemicarbazone derivatives bearing coumarin and D-galactose moieties with EGFR inhibitory activity and molecular docking study

Vu Ngoc Toan[1] · Nguyen Dinh Thanh[2]

Received: 5 May 2021 / Accepted: 19 July 2021 / Published online: 19 August 2021

Abstract

A series of substituted *N*-(2,3,4,6-tetra-*O*-acetyl-β-D-galactopyranosyl)thiosemicarbazones **5a–5j** of substituted 3-acetylcoumarins were synthesized with yields of 45–68%. All synthesized thiosemicarbazones were evaluated for cytotoxic activity against several cancer cell lines, such as human breast adenocarcinoma cells MCF7, human liver cancer cells HepG2, human cervical cancer cells HeLa, human melanoma cancer cells SK-Mel-2, and human lung cancer cells LU-1 by using the standard MTT assay. The IC_{50} values for these cancer cell lines were 1.28–11.81 μM (for MCF-7), 1.53–22.12 μM (for HepG2), 1.43–48.16 μM (for HeLa), 1.82–14.62 μM (for SK-Mel-2), and 1.74–14.62 μM (for LU-1). Most of the compounds were noncytotoxic against human WI-38 normal cell line ($IC_{50} > 16.9$ μM). The antiproliferative mechanisms were studied via EGFR inhibition and molecular docking. Docking studies revealed that there are strong interactions between a typical compound with the receptor of the EGFR tyrosine kinase domain with Erlotinib.

Graphical Abstract

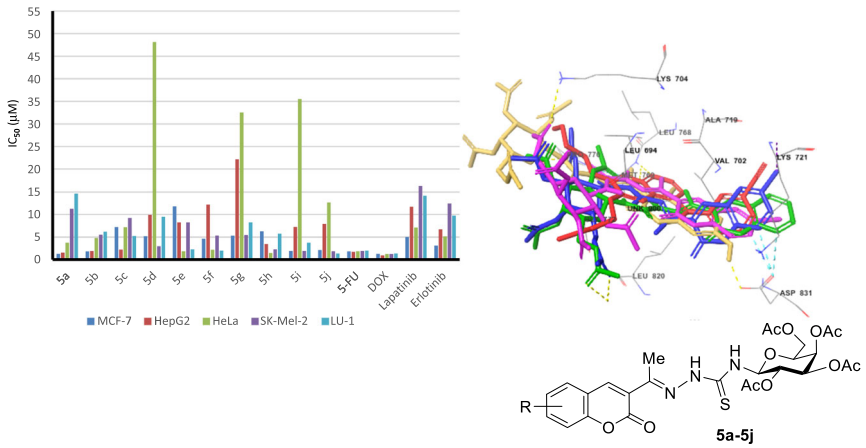

Keywords 3-Acetylcoumarins · Antiproliferative · D-galactose · EGFR tyrosine kinase · Thiosemicarbazones · Molecular docking

Supplementary information The online version contains supplementary material available at https://doi.org/10.1007/s00044-021-02773-y.

✉ Nguyen Dinh Thanh
nguyendinhthanh@hus.edu.vn

[1] Department of Toxicological Chemistry and Radiation, Institute for Advanced Technology, Vietnam Academy of Military Science and Technology, 17 Hoang Sam, Cau Giay, Ha Noi, Vietnam

[2] Faculty of Chemistry, VNU University of Science (Vietnam National University, Ha Noi), 19 Le Thanh Tong, Hoan Kiem, Ha Noi, Vietnam

Introduction

Coumarin is one of two important members of benzopyrone, including chromone (1-benzopyran-4-one, 4*H*-chromen-4-one) and coumarin (1-benzopyran-2-one, 2*H*-chromen-2-one). These rings constitute the core skeleton of many flavonoid compounds in nature [1]. These compounds bearing these rings possess diverse pharmacological activities [2], then they are used as the lead scaffolds in order to design, synthesize, and evaluate the new bioactive compounds having these rings [2]. Coumarin derivatives have different remarkable biological activity, such as antibacterial [3], antioxidant [4], and anticancer [5] activity, etc. Amongst various biological activities of compounds having coumarin rings, their anticancer activity is interested in cancer drug discovery [6]. They exhibit this activity *via* multiple different mechanisms and targets [7] and inhibit against different cancer cell lines, such as human liver cancer HepG2 [8], breast cancer MCF-7 [8], cervical carcinoma HeLa [9], melanoma SK-MEL-5 [10], etc. Figure 1 represents some representative examples that have anticancer activity. Geiparvarin, isolated from *Geijera parviflora*, demonstrates activity in the HL-60 and K562 cell lines with IC_{50} values of 6.3 and 9.2 μM, respectively [11]. Marmesin, isolated from *Gerbera anandria*, is found to have selective antitumor activities against HepG2 cells when tested against a panel of cancer cell lines [12]. Coumarin-hydrazone derivatives **A**, *N*′-(1-(4-dihydroxy-2-oxo-2*H*-chromen-3-yl)ethylidene)benzohydrazides, express IC_{50} values of 6.07 μM (R = OH) against human cervical cancer cells HeLa, of 7.79 μM (R = OH) and mammary gland adenocarcinoma cells MCF-7, and of 7.78 μM (R = H) against human lung adenocarcinoma cells A549 in comparison with IC_{50} values of standard drug Doxorubicin (7.01, 9.86, 6.22 μM, respectively) [13]. Compounds **B**, (*E*)-8-methoxy-3-(3-(4-methoxyphenyl)acryloyl)-2*H*-chromen-2-one, incorporating 3-methoxyphenyl moiety, displays the best anti-proliferative activity against HepG2 cells (with $IC_{50} = 0.65$ μM) [14]. Coumarin **C,** ethyl 1-((7-((4-nitrobenzyl)oxy)-2-oxo-2*H*-chromen-4-yl)methyl)piperidine-4-carboxylate, is the most potent counterpart against prostate DU145 and PC-3 cells with $IC_{50} = 8.95$ and 7.45 μM, respectively, with no toxic effect against non-tumorigenic cells [15].

Attaching the thiosemicarbazone group to the coumarin ring can elicit remarkable effects, most notably anti-cancer activity, such as anticancer [16], antibacterial [17], antifungal [18], antioxidant [19], and other activity. On the other hand, some thiosemicarbazones of substituted 3-acetyl coumarins are synthesized by their reaction with different thiosemicarbazides, and their properties (such as complex formations, spectral characteristics) have been studied and evaluated on their biological activity [19]. Some examples of these activities of coumarin thiosemicarbazones are displaying in Fig. 2. Compounds **D** express profound antiproliferative activity on MCF-7 (human breast cancer) and A549 (human lung carcinoma) cell lines [20]. Compounds **E** exhibit the inhibitory activity against the acetylcholinesterase enzyme [21].

Sugar moiety is used as a polar component in the design and synthesis of bioactive molecules, in general, and in thiosemicarbazones, in particular [16, 22]. Thiosemicarbazone having sugar moiety also exhibit various biological properties, such as antibacterial, antifungal, anticancer, and antioxidant activity [16, 23], etc. Figure 2 displays some examples of thiosemicarbazones bearing sugar moiety that have anticancer activity. Thiosemicarbazone **F** containing D-glucose moiety has remarkable antiproliferative activity against breast cancer

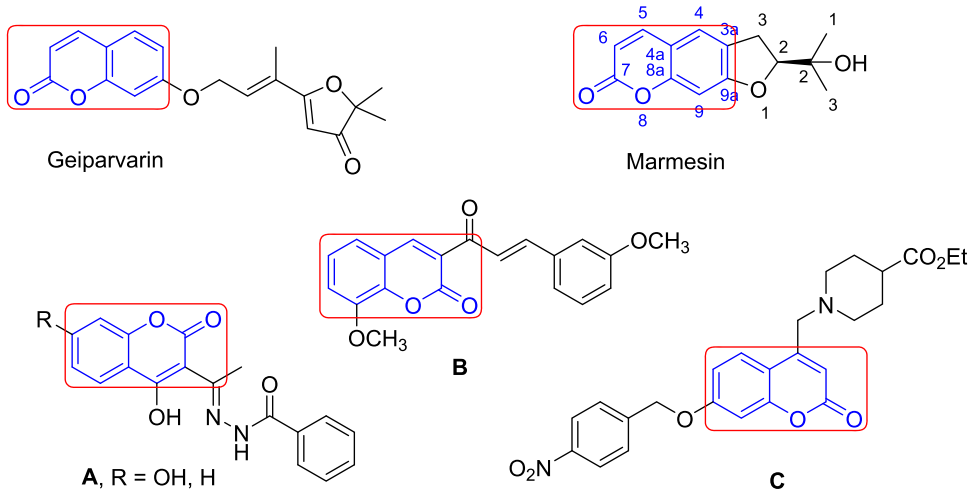

Fig. 1 Some coumarin compounds with anticancer activity having coumarin ring: Geiparvarin, Marmesin, (**A**), (**B**), and (**C**) moieties

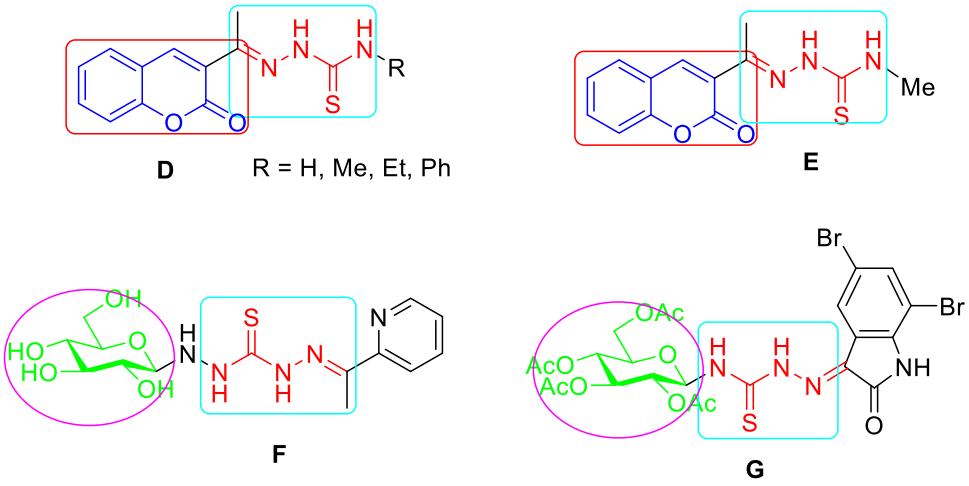

Fig. 2 Some bioactive thiosemicarbazones bearing coumarin (**D**), (**E**) and sugar (**F**), (**G**) moieties

cell line MDA-MB-231 and prostate cancer cell line PC-3 with IC_{50} values of 1.60 µM and 2.8 µM, respectively [16]. Compound **G** exhibits selective cytotoxicity against some cancer cell lines, such as LU-1, MCF7, HepG2, SW480, P338, and KB, with IC_{50} values of 2.75–12.75 µM [23].

It is known that epidermal growth factor receptor (EGFR) is a cell-surface receptor (a transmembrane protein) belonging to the ErbB family of receptor tyrosine kinase inhibitors (TKs) [24]. It is activated by binding of its specific ligands, including epidermal growth factor and transforming growth factor α (TGF-α), amphiregulin (AR), epiregulin (EREG), betacellulin (BTC), heparin-binding EGF (HB-EGF), and epigen (EPGN) [25]. EGFR has emerged as an important therapeutic target. EGFR is involved in cell proliferation and signal transduction and belongs to the human epidermal growth factor receptor (HER) family, including HER1 (erbB1, EGFR), HER2 (erbB2, NEU), HER3 (erbB3), and HER4 (erbB4) [26]. The EGFR pathway is responsible and plays an important role in promoting hepatocellular carcinoma (HCC) metastasis [27]. Overexpression of EGFR is frequently observed in HCC and EGFR activation has been proven to be a potential determinant of primary resistance of HCC cells to sorafenib, Erlotinib, therefore, this may explain the result of the most potent cytotoxic activity being displayed against the breast cancer cell line, MCF-7, compared to the other cell lines [28].

From the above discussions about the antiproliferative activity of compounds containing coumarin and monosaccharide moieties connected by thiosemicarbazone linker, we have performed the design, synthesis of some thiosemicarbazones having coumarin ring and D-galactose moieties (Fig. 3, Scheme 2). Their antiproliferative activity has been evaluated on some typical cancer cell lines and the interaction mode of the most active compounds would be estimated on the above-mentioned typical enzymes.

Results and discussion

Chemistry

Design of thiosemicarbazone derivatives

In the first step, substituted coumarin derivatives consisting of different substitutions like halogens, alkyl, hydroxyl, methoxy, and the combination of both methyl and hydroxyl groups were designed. In addition, the acetyl group was attached to position 3 of the coumarin ring. Thiosemicarbazide of D-galactose was also designed by addition acetyl group to all hydroxyl ones in sugar ring, then one of these acetyl groups was replaced by thiosemicarbazide. Next, thiosemicarbazone derivatives of coumarins were also designed by replacing the carbonyl group on the coumarin ring with the thiosemicarbazone linker. Schemes 1 and 2 display the reaction series in order to accomplish these designs.

Synthesis and characterization of thiosemicarbazone derivatives

The reaction of different substituted salicylaldehydes **1a**-**1f** with ethyl acetoacetate in the presence of piperidine (as the catalyst) led to producing corresponding substituted 3-acetylcoumarins **3a**-**3f** (Scheme $1_{(I)}$) [29–31]. The condensation process was carried out under ultrasound conditions at room temperature. 3-Acetyl-4-methylcoumarin (**3g**) was prepared by condensation reaction between *o*-hydroxy acetophenone and ethyl acetoacetate in the presence of piperidine (as the catalyst) under microwave-assisted reflux conditions for 40 min (Scheme $1_{(III)}$). Microwave power was 400 W. Another 3-acetyl coumarin, 3-acetyl-7-hydroxy-4-methylcoumarin (**3h**), was prepared from resorcinol by two-step synthesis: firstly, 7-hydroxy-4-methyl-2*H*-chromen-2-

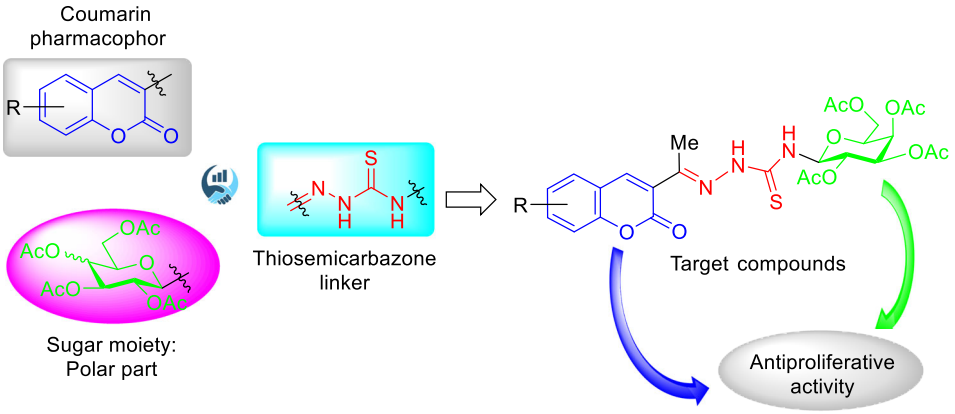

Fig. 3 Rationally designed coumarin−D-galactose hybrid compound through thiosemicarbazone linker and designed structures of synthesized hybrid compounds in this work

one (**1′h**) was produced by condensation of resorcinol with ethyl acetoacetate in 70% sulfuric acid [32]; after that, acetyl group was introduced into position 3 of coumarin ring by acetylation using glacial acetic acid in the presence of $POCl_3$ (Scheme $1_{(II)}$) [29].

Two other 3-acetyl-4-hydroxy coumarins (**3i**, R = H, and **3j**, R = 8-Me) were prepared by acetylation on position 3 of corresponding 4-hydroxy coumarins (**3′i,3′j**) using glacial acetic acid and PPA or acetyl chloride in pyridine. These coumarins were synthesized by two-step synthesis from phenol or *o*-cresol by treating them with Meldrum's acid to afford substituted 3-oxo-3-phenoxypropanoic acids **1′i,1′j**, respectively. By treating these acids with Eaton's reagent according to modified literature procedures, the mentioned-above coumarins (**3′i,3′j**) were obtained (Scheme 1_{IV} [29–31]). *N*-(2,3,4,6-Tetra-*O*-acetyl-β-D-galactopyranosyl)thiosemicarbazides (**4**) in Scheme 2 were prepared from corresponding isothiocyanates and 100% hydrazine hydrate using absolute ethanol as solvent using our previous procedure [23].

The condensation reaction between *N*-(2,3,4,6-tetra-*O*-acetyl-β-D-galactopyranosyl)-thiosemicarbazide (**4**) and substituted 3′-acetylcoumarin (**3a–3j**) resulted in the formation of corresponding thiosemicarbazones (**5a–5j**) (Scheme 2). We performed this reaction by using the microwave-assisted heating method (at the power of 400 W with irradiation times of 30–45 min). Both absolute methanol and ethanol could be used as a solvent for this process, but the former was favorable because thiosemicarbazide was easily soluble in methanol at room temperature but the target product did not dissolve, even at the reaction temperature. 3-Acetylcoumarins were dissolved with difficulty in these solvents in the same conditions, but they dissolved better under the reaction conditions (under microwave-assisted heating conditions). Therefore, absolute methanol was used favorably as a solvent for this reaction, and glacial acetic acid was applied as a catalyst. The obtained products were soluble better in hot ethanol, even 96% ethanol.

Spectral data, including IR and NMR spectra, supported the formation of the imine link in the target molecules **5a–5j**. The characteristic IR absorption band appeared at 1618–1603 cm^{-1} for >C=N bond, the carbon atom in this bond had a chemical shift at $\delta = 178.9–178.2$ ppm. The thiourea component in thiosemicarbazone linkage group (−NHCSNH−N=C<) was specified by characteristic IR absorption bands at $\nu = 3354–3447$ and 3328–3234 cm^{-1} (stretching vibrations of N−H bond), and by proton chemical shifts at $\delta = 11.36–11.02$ (singlet) and $\delta = 8.77–8.76$ ppm (doublet, $J = 6.5–7.0$ Hz) in ^1H NMR spectra for N–H groups.

Biological activity

In vitro cytotoxic activity

All synthesized thiosemicarbazones **5a–5j** were screened against four typical human cancer cell lines, including breast adenocarcinoma cells MCF7, liver cancer cells HepG2, cervical cancer cells HeLa, melanoma cancer cells SK-Mel-2, and lung cancer cells LU-1. The standard 3-(4,5-dimethylthiadiazol-2-yl)-2,5-diphenyltetrazolium bromide (MTT) assay was applied to determining cytotoxicity of these thiosemicarbazones [33]. Three reference drugs, including doxorubicin (DOX), Lapatinib, and Erlotinib, were used in these assays. Their IC_{50} values against each appropriate cancer cell line were presented in Table 1. The obtained IC_{50} values for all tested cancer cell lines were also listed in this table.

These IC_{50} values suggested that most of compounds **5a–5j** had remarkable cytotoxic activity to all of the tested cancerous cell lines. In general, our compounds were more selective towards MCF-7, HepG2, SK-Mel-2, and LU-1 than HeLa cell lines. Some compounds had good activity against tested cancer cell lines with $IC_{50} < 3$ μM, such as **5a**, **5b**, **5i**, and **5j** against MCF-7 cancer cell line, **5a**, **5b**, **5c**, and **5h** against HepG2, 5e, and 5h against HeLa, **5d**, **5h**, **5i**, and **5j**

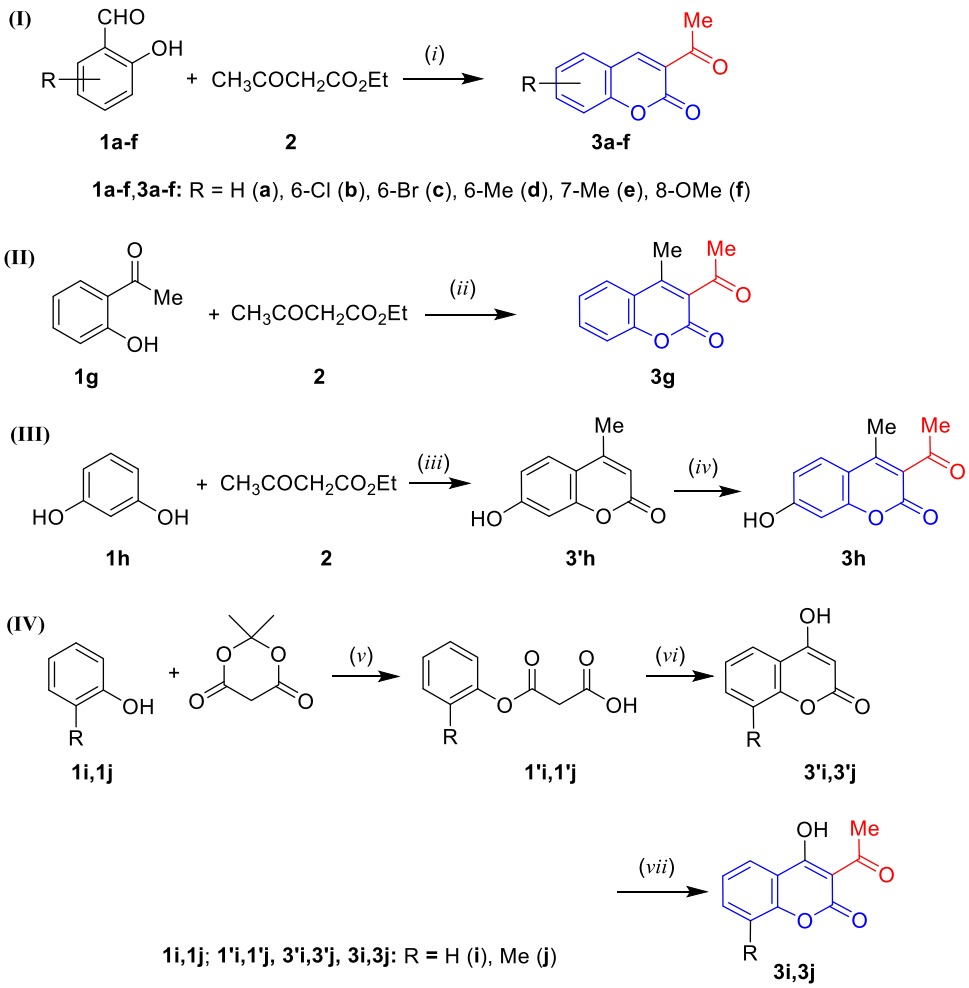

Scheme 1 Synthesis of some substituted 3-acetylcoumarins **3a**–**3j**. Reaction conditions: **I** (*i*) Piperidine, under ultrasound condition, 35 min, 25 °C. **II** (*ii*) Ethyl acetoacetate, CH_3COONa, under microwave-assisted conditions, 90 min, 400 W. **III** (*iii*) 70% Sulfuric acid, 0 °C then 25 °C, 24 h; (*iv*) Glacial acetic acid, $POCl_3$, under reflux, 90 min. **IV** (*v*) 90 °C, 5 h; (*vi*) Eaton's reagent, 70 °C, 1.5 h; (*vii*) Glacial acetic acid, $POCl_3$, under reflux, 50 min

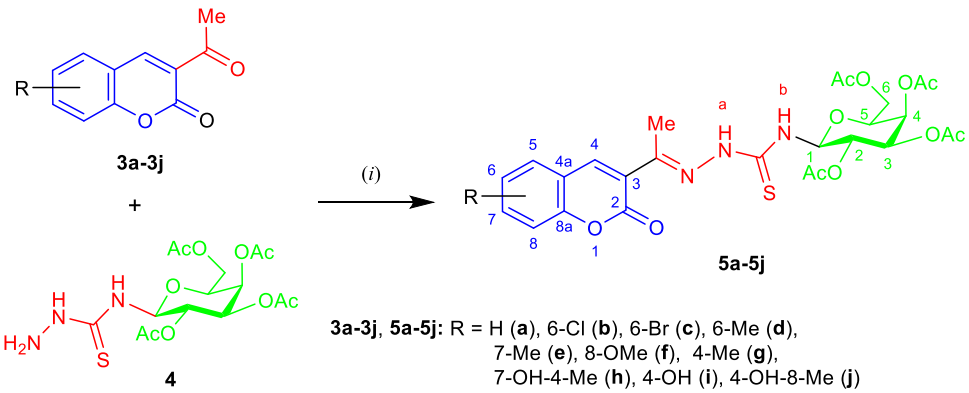

Scheme 2 Synthetic path to substituted 3-acetylcoumarin (tetra-*O*-acetyl-β-D-galactopyranosyl) thiosemicarbazones **5a**–**5j**. Reaction conditions: (*i*) Glacial acetic acid (catalyst), MeOH (solvent), 30−45 min. under MW-assisted conditions at 400 W

against SK-Mel-2, **5e**, **5f**, **5i**, and **5j** against LU-1 cancer cell lines. The order of the inhibitory effect against tested cancer cell lines was below. The comparison between the antiproliferative activity of our potent compounds and Doxorubicin was represented graphically in Fig. 4.

* MCF-7 cell lines: **5a** > **5b** > **5i** > **5j** > **5f** > **5d** > **5g** > **5h** > **5c** > **5e**, of which compound **5a** (R = H, IC_{50} = 1.28 µM) had the best activity in the series.

* HepG2 cell lines: **5a** > **5b** > 5c > **5h** > **5i** > **5j** > **5e** > **5d** > **5f** > **5g**. Compounds **5a** and **5b** showed the highest activity in this sequence (with IC_{50} values of 1.53 and 1.75 µM, respectively).

* HeLa cell lines: **5h** > **5e** > **5f** > **5a** > **5b** > **5c** > **5j** > **5g** > **5i** > **5d**, of which two compounds **5h** and **5e** had better antiproliferative activity against these cell lines (with IC_{50} values of 1.83 and 1.43 µM, respectively).

Table 1 Antiproliferative activity of thiosemicarbazones **5a–5j**

Compd.	R	IC_{50} (μM)					
		MCF-7	HepG2	HeLa	SK-Mel-2	LU-1	WI-38
5a	H	1.28 ± 0.08	1.53 ± 0.05	3.75 ± 0.24	11.25 ± 0.41	14.62 ± 0.18	325 ± 1.43
5b	6-Cl	1.81 ± 0.07	1.75 ± 0.07	4.79 ± 0.32	5.52 ± 0.21	6.21 ± 0.11	364 ± 1.49
5c	6-Br	7.18 ± 0.23	2.21 ± 0.08	7.16 ± 0.42	9.21 ± 0.32	5.24 ± 0.21	201 ± 1.35
5d	6-Me	5.18 ± 0.23	9.93 ± 0.12	48.16 ± 0.31	2.97 ± 0.08	9.52 ± 0.28	189 ± 1.56
5e	7-Me	11.81 ± 0.31	8.25 ± 0.12	1.83 ± 0.09	8.24 ± 0.42	2.25 ± 0.22	169 ± 1.28
5f	8-OMe	4.65 ± 0.32	12.21 ± 0.11	2.18 ± 0.19	5.31 ± 0.32	1.98 ± 0.08	287 ± 1.65
5g	4-Me	5.28 ± 0.42	22.12 ± 0.19	32.52 ± 0.31	5.47 ± 0.31	8.26 ± 0.32	227 ± 1.99
5h	7-OH-4-Me	6.28 ± 0.12	3.03 ± 0.15	1.43 ± 0.07	2.25 ± 0.08	5.73 ± 0.21	271 ± 1.46
5i	4-OH	1.92 ± 0.11	7.22 ± 0.09	35.52 ± 0.31	1.93 ± 0.07	3.75 ± 0.22	188 ± 1.87
5j	4-OH-8-Me	2.12 ± 0.11	7.92 ± 0.14	12.67 ± 0.32	1.82 ± 0.43	1.74 ± 0.07	210 ± 1.39
	DOX	1.28 ± 0.08	0.92 ± 0.06	1.27 ± 0.07	1.23 ± 0.07	1.34 ± 0.07	–
	Lapatinib	5.02 ± 0.17	11.71 ± 1.31	7.12 ± 0.17	16.32 ± 1.31	14.16 ± 1.31	–
	Erlotinib	3.11 ± 0.14	6.73 ± 0.33	5.15 ± 0.14	12.45 ± 0.33	9.75 ± 0.33	–

* SK-Mel-2 cell lines: **5j > 5i > 5h > 5d > 5f > 5g > 5b > 5e > 5c > 5a**. Compounds **5i** and **5j** also exhibited the highest activity in this sequence, with IC_{50} values of 1.93 and 1.83 μM, respectively.

* LU-1 cell lines: **5j > 5f > 5e > 5i > 5c > 5h > 5b > 5g > 5d > 5a**, in which compounds **5j** and **5f** expressed the highest cytotoxicity (with IC_{50} values of 1.74 and 1.98 μM, respectively).

Some conclusions on the structure-activity relationship of tested thiosemicarbazones could be drawn as follows. Both compounds **5a** (unsubstituted coumarin ring, R = H) and **5b** (having 6-chloro group) exhibited good inhibitory activity against two cancer cell lines MCF-7 and HepG2, whereas compound **5c** bearing bromo group on position 6 of coumarin ring inhibited only cancer cell line HepG2 and had unremarkable antiproliferative activity against MCF-7 cell line. Compounds **5i** and **5j** incorporating hydroxyl group at position 4 of coumarin ring, possessed strong antiproliferative activity against two investigated cell lines against MCF-7 and SK-Mel-2 cancer cell lines. Compound **5j** also exhibited strong activity against the LU-1 cancer cell line (IC_{50} = 1.74 μM) and bad activity against the HeLa cancer cell line. Replacement of H by other substituents, except chloro group, led to a decrease in the antiproliferative activity of synthesized compounds against MCF-7 and HepG2 cell lines. Attaching of methyl group alone at position 7 (in **5e**) or hydroxy and methyl groups at positions 7 and 4 (in **5h**) simultaneously on coumarin ring made this activity increase for HeLa cell lines, whereas hydroxy group alone on position 4 (in **5i**) or along with methyl group at position 8 (in **5j**) of coumarin ring increased the inhibitory activity against both SK-Mel-2 and LU-1 cell lines. The methyl group alone at positions 4, 6, or 7 on coumarin rings the worst inhibitory activity against HepG2, HeLa, and MCF-7 cell lines, respectively. Coumarin thiosemicarbazone (**5a**) had the worst inhibitions for two cancer cell lines SK-Mel-1 and LU-1.

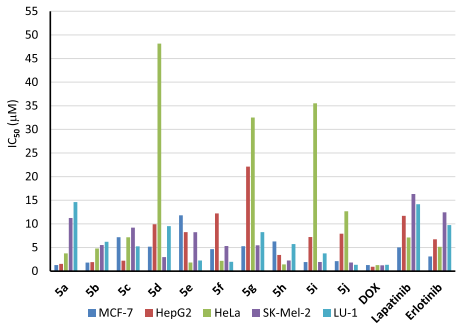

Fig. 4 Comparison between the antiproliferative activity of potent synthesized compounds **5a–5j** with DOX, Lapatinib, and Erlotinib

In order to evaluate the safety as a potential drug of all synthesized thiosemicarbazones **5a–5j**, their cytotoxicity on normal cells was determined for the human WI-38 normal cell line. The obtained investigation results showed that most of these compounds were noncytotoxic against this cell line with IC_{50} > 169 μM (Table 1), whereas the IC_{50} values against MCF-7 cell line were less than 1.28 μM, against HepG-2 cell line were less than 1.53 μM, against HeLa were less than 1.43 μM, against SK-Mel-2 were less than 1.82 μM, and against LU-1 cell line were less than 1.34 μM. Therefore, based on these obtained biological results, it means that the most active compounds on the non-cancerous cells were safe toward normal cells.

EGFR inhibition assay

In order to investigate the mode of antiproliferative activity of the synthesized compounds, the most active four compounds,

Table 2 IC_{50} values against EGFR

Compound	EGFR IC_{50} (μM)
5a	0.512
5b	0.258
5c	1.873
5h	1.624
Lapatinib	0.063
Erlotinib	0.105

Table 3 Inhibitory activities of compounds **5a** and **5b** against EGFR-TKs

Compound	IC_{50} (μM)	
	EGFR-L858R-TK	EGFR-T790M-TK
5a	102.63 ± 0.34	461.61 ± 3.12
5b	85.92 ± 0.32	432.65 ± 2.91
Lapatinib	61.16 ± 0.26	377.42 ± 5.23
Erlotinib	91.23 ± 0.41	422.17 ± 2.66

5a, **5b**, **5c**, and **5h** against HepG2 cancer cell line were further subjected to EGFR kinase activity assay [34, 35]. Lapatinib and Erlotinib were used as standard drugs (which inhibit EGFR) [36] and the HepG2 cancer cells were used for this test. The obtained results were displayed in Table 2.

The biological data in this table showed that compounds **5a** and **5b** had better inhibitory activity than the two remained ones, but worse activity than standard drugs, Lapatinib and Erlotinib. So, these compounds were chosen for further evaluation of their inhibition effect against other types of EGFR tyrosine kinase, EGFR T790M-TK, and EGFR L858R-TK. The inhibitor activities of compounds **5a** and **5b** against EGFR-L858R- and EGFR-T790M-tyrosine kinases were displayed in Table 3. The potent compounds **5a** and **5b** showed about two-third of the activities of Lapatinib on the two types of mutants. Compound **5a** showed activity near to Erlotinib but less than Lapatinib. Also, compound **5b** showed activity near Lapatinib and had better activity than Erlotinib and better than compound **5a**.

Annexin V-FITC apoptosis assay

The programmed cell death in biological systems included autophagy, necrosis, and apoptosis [9, 14, 15]. Apoptosis is a series of biochemical events leading to morphological changes and cell death. It is known that many cytotoxic drugs show anticancer activities by inducing cell apoptosis. To further understand the antiproliferative mechanism of compounds **5a** and **5b**, their effects on cell cycle progression in HepG2 cells were examined (at the IC_{50} of this cell line) using the flow cytometry method with annexin V/propidium iodide double staining [34].

Table 4 Percent of cell death induced by compounds **5a** and **5b** on HepG2 cells (in %)

Compound	Apoptosis		Necrosis	Total
	Early	Late		
5a	7.38	12.61	9.15	29.14
5b	6.42	18.65	12.54	37.61
Control	0.28	0.16	1.43	1.87

The obtained results presented in Table 4 showed that compounds **5a** and **5b** had the ability to induce apoptosis at early, late apoptotic stages and necrosis development, compared to untreated control. In the early stage, the apoptosis percentages induced by compounds **5a** and **5b** were 7.38 and 6.42%, respectively whereas the apoptosis percentage of control (0.1% DMSO) was 0.28%. In the late stage, compared to control, the apoptosis cells percentages of tested compounds **5a** and **5b** were increased to 12.61 and 18.65%, respectively. In addition, the necrosis cells percentages were changed remarkably, reaching 9.15 and 12.54%, respectively. These two compounds increased cell population at the early apoptotic stage by 26.36 and 22.93 folds, respectively, compared to control cells. Interestingly, these compounds significantly increased the late apoptotic cell population by 78.81 and 116.56 folds, respectively, compared to control cells. In addition, compounds **5a** and **5b** significantly increased cell necrosis by 6.40 and 8.77 folds, respectively, compared to control cells. The total apoptosis (including the early and late stages) and necrosis percentages were 29.14 and 37.61%, respectively, indicated that the treatment of HepG2 cells with compounds **5a** and **5b** leading to an increase in the apoptotic cells percentages from 1.87% to 29.14 and 37.61%, respectively. It is clear that the tested compounds, **5a**, and **5b**, caused remarkable apoptosis in the HepG2 cell line. Finally, the potential antiproliferative activity together with EGFR inhibitory activity exerted by compounds **5a** and **5b** prompted us to discover their possible binding interactions with EGFR active sites by carrying out a molecular docking study.

Molecular docking

A molecular docking study was carried out to obtain a better understanding of EGFR higher inhibitory activity results of compounds **5a**, **5b**, **5c**, and **5h** in order to rationalize and describe their binding mode into EFGR active site. It's known that Erlotinib was a tyrosine kinase inhibitor used to block EGFR signaling in cancer. This drug exhibited its activity thought to bind the active conformation of the EGFR-TKD (tyrosine kinase domain) [35]. The target for docking simulations was the crystallographic structure of

Table 5 Molecular docking analysis of protein target 4HJO with selected compounds **5a**, **5b**, **5c**, **5h** in comparison with Erlotinib

Compd.	Binding free energy (kcal/mol)	Hydrogen bonding
5a	−6.847	+) C=O group of the 6-acetyl group with HS group of cysteine (residue Cys773, $l = 2.30$ Å).
		+) Oxygen atom of C−O bond in 4-acetyl with 2-amino group of cysteine (residue Cys773, $l = 2.71$ Å).
		+) C=O group of coumarin ring with a 2-amino group of methionine (residue Met769) ($l = 2.00$ Å).
		+) Aromatic H-bonding of the oxygen atom of 3-OH group in threonine (residue Thr766) with hydrogen atoms H-4 and H-5 of coumarin ring ($l = 3.28$ and 3.50 Å, respectively) and of C=O carboxylate of asparagine (residue Asp831) with hydrogen atom H-8 of coumarin ring ($l = 3.16$ Å).
5b	−6.804	+) C=O group of 6-acetyl with HS group of cysteine (residue Cys773, $l = 2.15$ Å).
		+) Oxygen atom of pyranose ring with a 2-amino group of cysteine (residue Cys773, $l = 2.65$ Å).
		+) C=O group of 3-acetyl with 2-amino group of lysine (residue Lys692, $l = 2.33$ Å).
		+) C=S of thiosemicarbazone with a 2-amino group of methionine (residue Met769, $l = 2.44$ Å).
		+) Chloro substituent with a 2-amino group of lysine (residue Lys721, $l = 3.00$ Å)
5c	−6.760	+) C=O group of 6-acetyl with 2-amino group of lysine (residue Lys692, $l = 2.60$ Å) and with a 2-amino group of lysine (residue Lys704, $l = 2.17$ Å).
		+) Aromatic H-bonding of C=O carboxylate asparagine (residue Asp831) with hydrogen atom H-7 of coumarin ring ($l = 3.31$ Å).
5h	−6.256	+) 7-OH group of coumarin ring with the negative-charged oxygen atom of carboxylate group of asparagine (residue Asp831, $l = 1.96$ Å).
		+) NH group of hydrazone moiety with a 2-amino group of methionine (residue Met769, $l = 2.18$ Å).
		+) NH group of thiourea moiety with C=O carboxyl group of Proline (residue Pro770, $l = 2.71$ Å).
Erlotinib	−8.984	+) Nitrogen atom N-1 of quinazoline with a 2-amino group of methionine (residue Met769, $l = 1.96$ Å).
		+) Oxygen atom of terminal methoxy group of Erlotinib with 2-amino group of cysteine (residue Cys773, $l = 2.00$ Å).
		+) Aromatic H-bonding of oxygen atom in C=O of methionine with hydrogen atom H-2 of Erlotinib (residue Met769, $l = 3.23$ Å).
		+) Aromatic H-bonding of oxygen atom in C=O carboxylic of glutamine with hydrogen atom H-8 of Erlotinib (residue Gln767, $l = 3.38$ Å).

EGFR (see "Molecular docking"). The free energies and binding mode of the selected (most active against HepG2 cell) compounds **5a**, **5b**, **5c**, and **5h** with EGFR in comparison with Erlotinib were performed through Schrödinger software [37] and represented in Table 5. Compounds 5 consisted of two different parts in terms of polarity: two coumarin ring was the non-polar part, while the sugar moiety was the polar one. The docking results revealed that the compounds **5a**, **5b**, **5c**, and **5h** had similar orientations inside the ATP binding site (Fig. 5) as Erlotinib was in this active site. Table 5 also displayed the molecular docking analysis of protein target 4HJO with selected compounds **5a**, **5b**, **5c**, **5h** in comparison with Erlotinib. As shown in this table, the designed thiosemicarbazone derivatives showed good binding energies (from −6.847 to −6.256 kcal/mol), compared with the energy binding of Erlotinib that was −8.984 kcal/mol. Figure 5 displayed **t**he 2D interactions with EGFR of selected compounds and Erlotinib and Fig. 6 represented the 3D interactions with EGFR of these ligands.

Figure 5 displayed some important and responsible active interactions, including hydrophilic and hydrophobic ones, which took place when the tested bioactive compounds approached the active site (at the binding cavity of EGFR tyrosine kinase domain). For example, compound **5a** formed two hydrogen bonds only with amino acid residue cysteine Cys773, and hydrophobic interactions at the hydrophobic cavity containing six amino acid residues, including six amino acid residues Leu753, Leu764, Thr766, Leu768, Met769, and Pro779. Other hydrophobic interactions were also found to occur at the hydrophobic cavity containing three amino acid residues, including three amino acid residues Thr830, Asp831, and Leu834 (Figs. 5A and 6A). Compound **5b** formed five hydrogen bonds with four amino acid residues Lys721, Met769, Cys773, and Lys692, and hydrophobic interactions at the hydrophobic cavity containing four amino acid residues Leu764, Ile765, Thr766, Leu768. Other hydrophobic interactions were also found to occur at the hydrophobic cavity containing three amino acid residues Thr830, Asp831, and Leu834 (Figs. 5B and 6B). Compound **5c** formed two hydrogen bonds with two amino acid residues Lys692 and Lys705, and hydrophobic interactions at the hydrophobic cavity containing four amino acid residues Leu764, Thr766, Gln767, Leu768.

(A) **5a** (R=H)

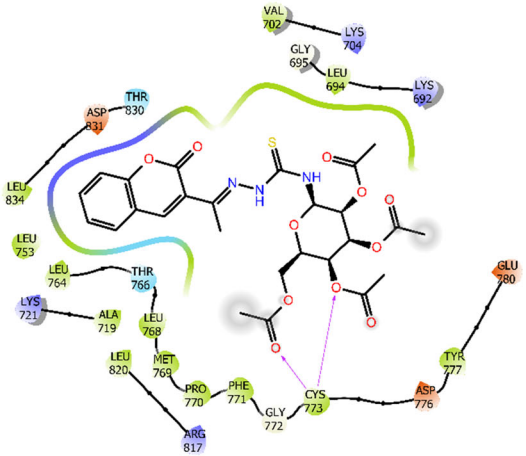

(B) **5b** (R = 6-Cl)

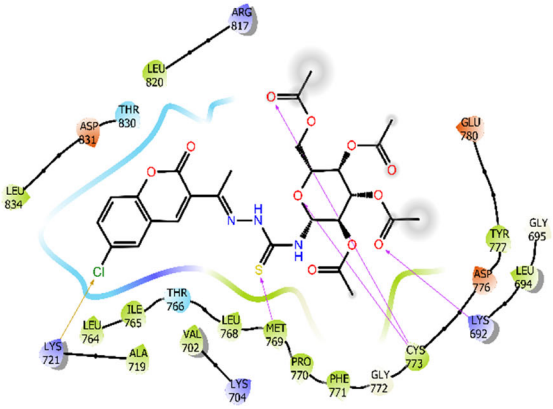

(C) **5c** (R = 6-Br)

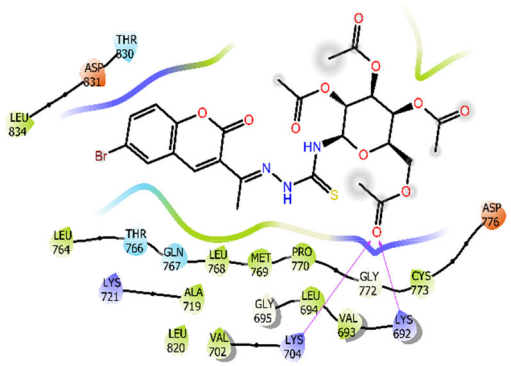

(D) **5h** (R = 7-OH-4-Me)

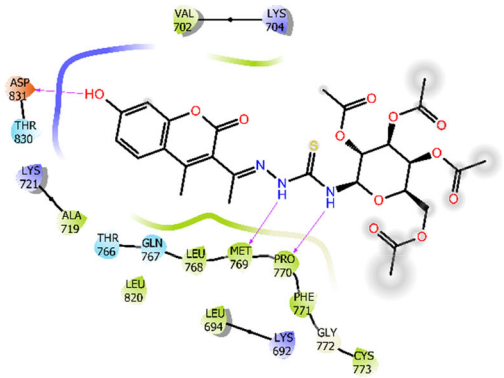

(E) Erlotinib

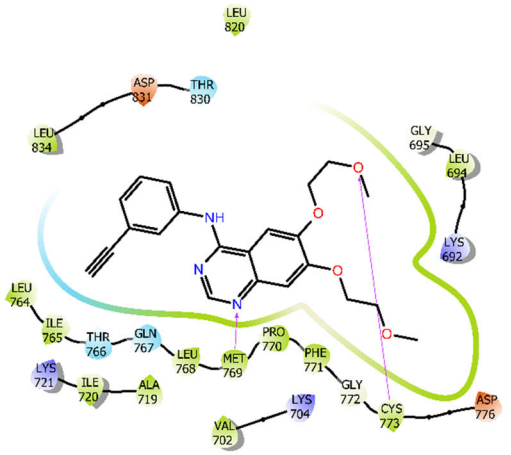

Legends

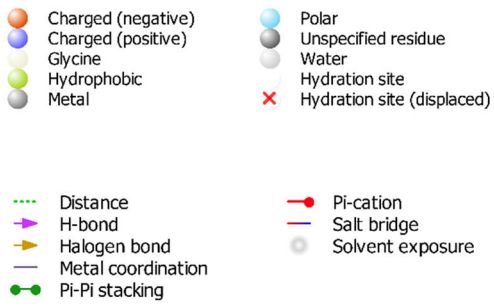

Fig. 5 The 2D interactions with EGFR of compound **5a** (**A**), of compound **5b** (**B**), of compound **5c** (**C**), of compound **5h** (**D**), and Erlotinib (**E**)

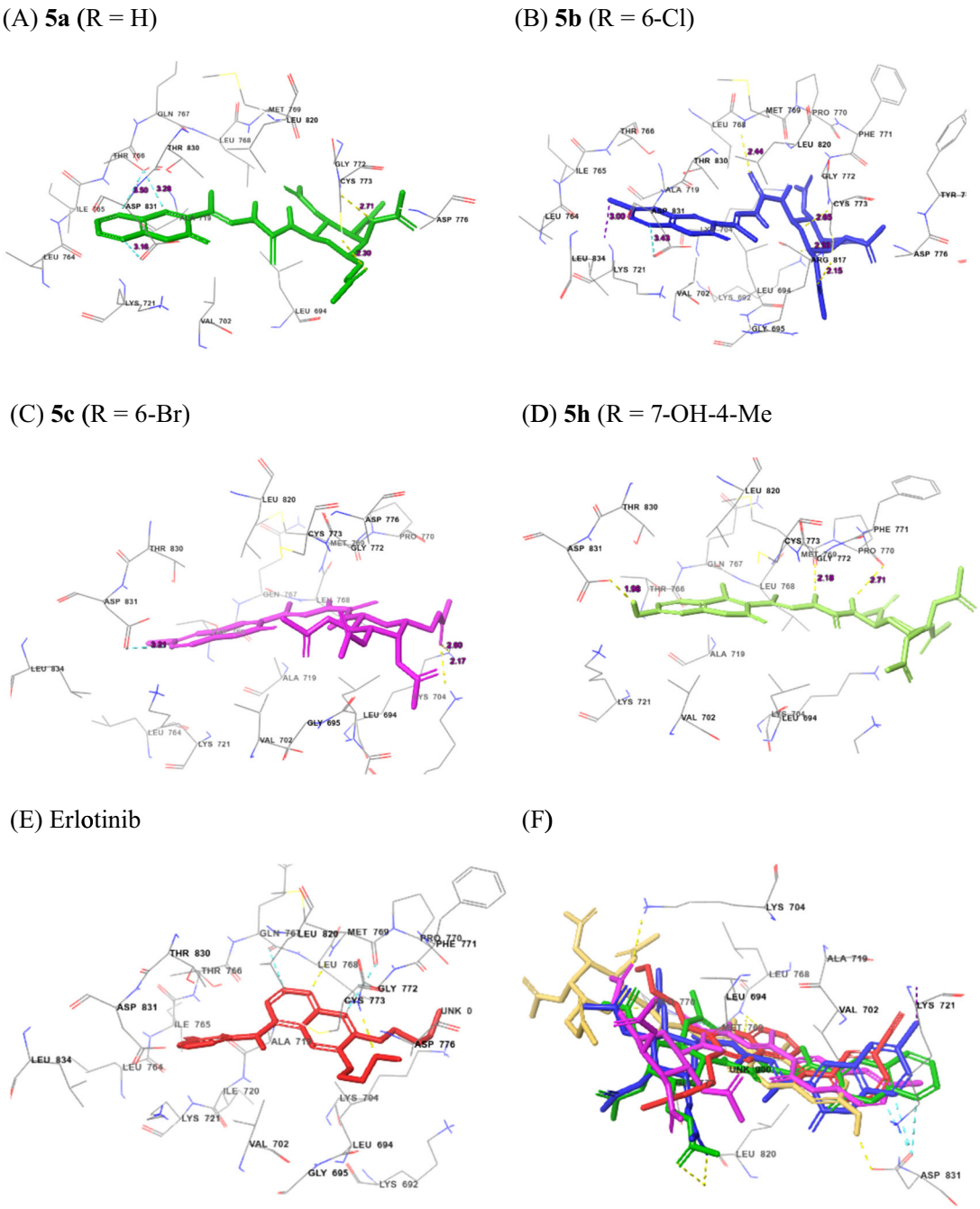

Fig. 6 The 3D interaction with EGFR of compound **5a** (**A**), of compound **5b** (**B**), of compound **5c** (**C**), of compound **5h** (**D**), and Erlotinib (**E**). Section (**F**) displayed the superimpositions of Erlotinib (red), **5a** (green), **5b** (blue), **5c** (magenta) and **5h** (orange) in receptor cavity

Other hydrophobic interactions were also found to occur at the hydrophobic cavity containing three amino acid residues Thr830, Asp831, and Leu834 (Figs. 5C and 6C). Compound **5h** formed three hydrogen bonds with three amino acid residues Met769, Pro770, and Asp831, and hydrophobic interactions at the hydrophobic cavity containing four amino acid residues Leu764, Thr766, Gln767, Leu768. Other hydrophobic interactions were also found to occur at the hydrophobic cavity containing three amino acid residues Thr830, Asp831, and Leu834 (Figs. 5D and 6D). As shown in Figs. 5 and 6, quinazoline moiety of Erlotinib was inserted into the adenine pocket of the EGFR receptor and its nitrogen atom number 1 formed a hydrogen bond with Met769 with bond length 1.96 Å. Erlotinib formed two hydrogen bonds with Met769 and Cys773, and hydrophobic interactions at the hydrophobic cavity containing five amino

acid residues Leu764, Ile765, Thr766, Gln767, Leu768. Other hydrophobic interactions were also found to occur at the hydrophobic cavity containing three amino acid residues Thr830, Asp831, and Leu834 (Figs. 5E and 6E). The binding energy values and the hydrogen-bond binding in Table 5 showed that the hydrogen-bond binding of the C=O group of 6-acetyl with HS group of cysteine (residue Cys773) played the important role in the docking interactions of selected ligands with the active site of EGFR receptor. Besides, ligand **5a** (R = H) had additional hydrogen-bond binding of C=O group of coumarin ring with a 2-amino group of methionine (residue Met769), and aromatic H-bonding of the oxygen atom of 3-OH group in threonine (residue Thr766) with hydrogen atoms H-4 and H-5 of coumarin ring, and of C=O carboxylate of asparagine (residue Asp831) with hydrogen atom H-8 of coumarin ring. It is these interactions that enhance the active interaction of **5a** with EGFR receptors.

As shown in Table 5, Figs. 3 and 4, D-galactopyranose and coumarin moieties of compounds **5a** and **5b** inserted better into the adenine pocket of the EGFR receptor. This increases the EGFR inhibitory activity of compounds **5a** and **5b**. Both of these compounds have hydrogen-bonding interactions with amino acids just as Erlotinib did. These binding interactions may be responsible for the EGFR inhibitory potency of these compounds. In addition, compound **5b** formed a hydrogen bond with lysine Lys721, which possibly makes its inhibitory activity higher than that of compound **5a**. However, in cases of compounds **5c** and **5h**, the absence of these hydrogen-bonding interactions with the key amino acid residue in the ATP binding site could explain the decrease in IC_{50} of ligands **5c** and **5h**. Thus, compounds **5a** and **5b** had a similar binding mode like Erlotinib on the EGFR enzyme and have good binding energies. Amongst hydrophilic and hydrophobic interactions at the active site of the EGFR enzyme, the hydrogen-bond bindings between acetate function and appropriate amino acid residues contributed the most in intensifying their potency against this enzyme.

Conclusions

Thiosemicarbazones **5a**–**5j** bearing coumarin and D-galactose moieties were produced from appropriate 3-acetyl derivatives and thiosemicarbazide, respectively. The microwave-assisted method showed the efficient and convenient method for the synthesis of these thiosemicarbazones. These compounds exhibited potent antiproliferative activity against tested cancer cells, including MCF7, HepG2, HeLa, SK-Mel-2, and LU-1. Amongst tested compounds, **5a** and **5b** showed good activity against EGFR-L858R and EGFR-T790M tyrosine kinase. From the results of the annexin VFITC apoptosis assay, it is clear that the treatment of HepG2 cells with compounds **5a** and **5b** causing to increase in apoptotic cells percentage, and these compounds induced apoptosis in the HepG2 cell line. The resulted docking studies showed that compounds **5a**, **5b**, **5c**, **5h** had similar binding modes to Erlotinib on the EGFR enzyme and have good binding energies. Amongst hydrophilic and hydrophobic interactions at the active site of the EGFR enzyme, the hydrogen-bond bindings between acetate function and appropriate amino acid residues had the most important contribution in intensifying their potency against this enzyme.

Experimental

Melting points were determined by the open capillary method on STUART SMP3 instrument (BIBBY STERILIN, UK) and are uncorrected. IR spectra (KBr disc) were recorded on an Impact 410 FT-IR Spectrometer (Nicolet, USA). ^{1}H and ^{13}C NMR spectra were recorded on Bruker Avance Spectrometer AV500 (Bruker, Germany) at 500 MHz and 125 MHz, respectively, using DMSO-d_6 as solvent and TMS as an internal standard; ESI/HR-mass spectra were recorded on LC-ESI-HRMS LTQ Orbitrap XL or Thermo Scientific Exactive Plus Orbitrap spectrometers (ThermoScientific, USA) in methanol using ESI method. The analytical thin-layer chromatography (TLC) was performed on silica gel 60 $WF_{254}S$ aluminum sheets (Merck, Germany) and was visualized with UV light. Chemical reagents in high purity were purchased from the Merck Chemical Company (in Viet Nam). All materials were of reagent grade for organic synthesis.

Synthesis of substituted 3-acetylcoumarins (3a–3j)

Synthesis of substituted 3-acetylcoumarins (3a–3h) from substituted salicylaldehydes under ultrasound irradiation

General procedure Appropriately substituted salicylaldehydes (**1a**–**1h**, 10 mmol), ethyl acetoacetate (2, 15 mmol, 1.95 g, 1.91 mL) were dissolved in methanol (5 mL). To this mixture piperidine (1 mol%, 0.01 mL) was added. The reaction mixture was irradiated under ultrasound conditions at room temperature for a suitable time (see Table 1), then cooled to room temperature. The precipitate was collected by suction filtration, washed with cold methanol (2 × 5 mL), and recrystallized from 96% ethanol to afford substituted 3-acetylcoumarins (**3a**-**h**).

3-Acetylcoumarin (3a) From salicylaldehyde **1a** (R = H, 10 mmol, 1.0 mL), ethyl acetoacetate 2 (15 mmol, 1.9 mL). Yield: 1.5 g (79%, method B); 1.7 g (92%, method C) of **3a**

as shining yellow crystals. M.p.: 119−120 °C, ref.: 119 −120 °C [38]. IR (KBr, cm^{-1}): 1738 ($\nu_{C=O}$ ketone), 1675 ($\nu_{C=O}$ lactone), 1610, 1595 and 1551 ($\nu_{C=C}$ arene), 1214 and 1085 (ν_{COC}).

3-Acetyl-6-chlorocoumarin (3b) From 5-chlorosalicylaldehyde **1b** (10 mmol, 1.57 g), ethyl acetoacetate 2 (10 mmol, 1.30 g, 1.24 mL). Yield: 1.16 g (52%, method A), 1.85 g (83%, method B), 2.07 g (93%, method C) of **3b** as yellow needle crystals. M.p.: 204 −205 °C, ref.: 206 °C [39]. IR (KBr, cm^{-1}): 1736 ($\nu_{C=O}$ ketone), 1676 ($\nu_{C=O}$ lactone), 1610, 1596 and 1552 ($\nu_{C=C}$ arene), 1204 and 1083 (ν_{COC}).

3-Acetyl-6-bromocoumarin (3c) From 5-bromosalicylaldehyde **1c** (10 mmol, 2.01 g), ethyl acetoacetate 2 (10 mmol, 1.30 g, 1.24 mL). Yield: 1.47 g (55%, method A), 2.24 g (84%, method B), 2.51 g (94%, method C) of **3c** as lemon yellow needle crystals. M.p.: 221−222 °C, ref.: 220−221 °C [38]. IR (KBr, cm^{-1}): 1742 ($\nu_{C=O}$ ketone), 1675 ($\nu_{C=O}$ lactone), 1596, 1546 and 1504 ($\nu_{C=C}$ arene), 1211 and 1109 (ν_{COC} lactone).

3-Acetyl-6-methylcoumarin (3d) From 5-methylsalicylaldehyde **1d** (10 mmol, 1.36 g), ethyl acetoacetate 2 (10 mmol, 1.30 g, 1.24 mL). Yield: 0.95 g (47%, method A), 1.42 g (70%, method B), 1.82 g (90%) of **3d** as lemon yellow needle crystals. M.p.: 127–128 °C, ref.: 127.5–128.3 °C [38]. IR (KBr, cm^{-1}): 1740 ($\nu_{C=O}$ ketone), 1675 ($\nu_{C=O}$ lactone), 1597, 1548, and 1504 ($\nu_{C=C}$ arene), 1212 and 1109 (ν_{COC} lactone).

3-Acetyl-7-methylcoumarin (3e) From 4-methylsalicylaldehyde **1e** (0 mmol, 1.36 g), ethyl acetoacetate 2 (10 mmol, 1.30 g, 1.24 mL). Yield: 0.95 g (47%, method A), 1.42 g (70%, method B), 1.82 g (90%) of **3e** as lemon yellow needle crystals. M.p.: 160−161 °C, ref.: 160−161 °C [40]. IR (KBr, cm^{-1}): 1741 ($\nu_{C=O}$ ketone), 1676 ($\nu_{C=O}$ lactone), 1597, 1546 and 1504 ($\nu_{C=C}$ arene), 1211 and 1109 (ν_{COC} lactone).

3-Acetyl-8-methoxycoumarin (3f) From *ortho*-vanillin **1f** (3-methoxysalicylaldehyde, R = 3-OMe, 10 mmol, 1.52 g), ethyl acetoacetate 2 (10 mmol, 1.30 g, 1.24 mL). Yield: 1.42 g (65%, method A) of **3f** as pale-yellow needle crystals. M.p.: 173−174 °C, ref.: 172 °C [41]. IR (KBr, cm^{-1}): 1734 ($\nu_{C=O}$ ketone), 1685 ($\nu_{C=O}$ lactone), 1601, 1567 and 1472 ($\nu_{C=C}$ arene), 1200 and 1091 (ν_{COC} lactone).

Synthesis of 3-acetyl-4-methylcoumarin (3g) from o-hydroxyacetophenone

A reaction mixture consisted of *o*-hydroxyacetophenone (**1g**, 0.1 mol, 13.6 g, 1.20 mL), and ethyl acetoacetate (0.15 mol, 19.5 g, 18.6 mL). Anhydrous sodium acetate (0.15 mol, 12.5 g) was added and the mixture was heated under microwave-assisted conditions of 400 W for 90 min, then cooled to room temperature. The reaction mixture was poured into ice water, separated yellow precipitate was collected by suction filtration, washed with cold methanol (2 × 5 mL), and recrystallized from 96% ethanol to afford 3-acetyl-4-methylcoumarin (**3g**) as yellow needle crystals. Yield: 0.81 g (40%). M.p.: 101−103 °C, ref.: 101−103 °C [42]. IR (KBr, cm^{-1}): 1742 ($\nu_{C=O}$ lactone), 1616 ($\nu_{C=N}$), 1522 and 1495 ($\nu_{C=C}$ arene), 1372 ($\nu_{C=S}$), 1224 & 1062 (ν_{COC} ester).

Synthesis of 3-acetyl-7-hydroxy-4-methylcoumarin (3h) from resorcinol

A mixture of resorcinol (**1h**, 0.1 mol, 11.0 g) and ethyl acetoacetate (0.015 mol, 19.5 g, 18.6 mL) in 70% sulfuric acid (75 mL) was heated on a water bath at 70 °C for 3 h. The resulting reddish-brown colored solution was decomposed with crushed ice (150 g). The separated bright yellow-colored solid was filtered, washed with an excess of cold water, dried, and crystallized from methanol to get the pure product, 4-methyl-7-hydroxycoumarin (**1′h**) as dark brown crystals. Yield: 22.6 g (85%). M.p. 184−185 °C, refs.: 185 °C [32], 189–191 °C [38].

Compound **1′h** (37 mmol, 6.51 g) was dissolved in glacial acetic acid (56 mmol, 3.36 g, 3.23 mL). To this solution, $POCl_3$ (12 mmol, 1.84 g, 1.12 ml) was added. The reaction mixture was heated under reflux for 90 min, then was allowed to cool to room temperature, poured onto crushed ice, collected the solid product by suction filtration, washed with water, dried at room temperature, and recrystallized from a mixture of 96% ethanol and toluene (4:1 by volume) to afford 3-acetyl-4-methyl-7-hydroxycoumarin (**3h**) as yellowish solids. Yield: 4.84 g (60%). M.p.: 157 −159 °C. IR (KBr, cm^{-1}): 1742 ($\nu_{C=O}$ lactone), 1616 ($\nu_{C=N}$), 1522 and 1495 ($\nu_{C=C}$ arene), 1372 ($\nu_{C=S}$), 1224 & 1062 (ν_{COC} ester); ^{1}H NMR (500 MHz, DMSO-d_6), δ (ppm): 7.81 (d, J = 8.5 Hz, 1H, H-5), 7.25 (d, J = 2.3 Hz, 1H, H-8), 7.16 (dd, J = 8.75, 2.25 Hz, 1H, H-6), 6.39 (d, J = 1.0 Hz, 1H, H-8), 2.31 (s, 3H, C=NCH_3).

Synthesis of substituted 3-acetyl-4-hydroxycoumarins (3i and 3j)

These 3-acetyl derivatives of coumarins were synthesized according to literature procedures [29–31] with some modifications. A mixture of phenol (1i) or *o*-cresol (1j) (20 mmol) and Meldrum's acid (20 mmol, 3.17 g) was stirred at 90 °C for 5 h, then cooled to room temperature. Ethyl acetate and saturated sodium bicarbonate solution were added to the reaction mixture. The separated aqueous layer was acidified to pH = 1−2 with conc. HCl and extracted with methylene chloride several times. The combined extracts were dried

over $CaCl_2$ and concentrated to give crude compounds 1′i or 1′j, respectively, that enough pure for the next conversion.

A mixture of **1′i** or **1′j** and Eaton's reagent (30 mL) was stirred at 70 °C for 1.5 h and then water was added to this mixture while stirring vigorously. The precipitate was filtered by suction, washed with water, and dried in air to give the yellow solids, which were recrystallized from 96% ethanol to afford title compounds **3′i** or **3′j**, respectively. These compounds were converted into corresponding 3-acetyl derivatives **3i** or **3j**, respectively, by using the above-mentioned procedure for the synthesis of 3-acetyl-4-methyl-7-hydroxycoumarin **3h**.

4-Hydroxycoumarin (3′i, R = H) From phenol **1i** (20 mmol, 1.88 g). Yield: 2.44 g (75%) as pale-yellow crystals. M.p. 210−212 °C, ref.: 213.0−214.3 °C [30].

4-Hydroxy-8-methylcoumarin (3′j, R = Me) From *o*-cresol **1j** (20 mmol, 2.16 g). Yield: 2.46 g (70%) as yellow solids. M.p. 231−232 °C, refs.: 231.1−233.4 °C [30].

3-Acetyl-4-hydroxycoumarin (3i) From coumarin **3′i** (10 mmol, 1.62 g). Yield: 1.43 g (70%) of **3j** as pale-yellow crystals. M.p. 133−135 °C, refs.: 133−135 °C [29].

3-Acetyl-4-hydroxy-8-methylcoumarin (3j) From coumarin **3′j** (20 mmol, 2.16 g). Yield: 1.48 g (68%) of **3j** as yellow solids. M.p. 115−117 °C, ref.: 116 °C [43].

General procedure for the synthesis of substituted 3-acetylcoumarin *N*-(2,3,4,6-tetra-*O*-acetyl-β-D-galactopyranosyl)thiosemicarbazones (5a–5j)

A suspension mixture consisted of appropriate substituted 3-acetylcoumarins (**3a**–**3j**, 1 mmol) and *N*-(2,3,4,6-tetra-*O*-acetyl-β-D-galactopyranosyl)thiosemicarbazide (**4**, 1 mmol) in methanol (5 mL). Glacial acetic acid (0.05 mL) was added to this mixture. The reaction was performed by irradiating under reflux for 30 min in a home-hold microwave oven. After irradiating for 30−45 min, the suspension mixture became a clear solution. The irradiation was continued in the given time. At the end of the reaction, the precipitate has appeared. The reaction mixture was cooled to room temperature; the colorless precipitate was filtered with suction. The crude product was recrystallized from 95% ethanol or toluene: ethanol (1:1 in volume) to afford the title compounds **5a**–**5j**.

3-Acetylcoumarin *N*-(2,3,4,6-tetra-*O*-acetyl-β-D-galactopyranosyl)thiosemicarbazone (5a)

From **3a** (1 mmol, 188 mg) and 4 (1 mmol, 421 mg). Microwave irradiation time: 45 min. Yield: 266 mg (45%) of **5a** as pale-yellow crystals from 96% ethanol. M.p.: 114−115 °C; $[\alpha]_D^{25}$ +77.8 (*c* 0.23, $CHCl_3$). IR (KBr), ν (cm^{-1}): 3354 and 3332 (ν_{NH} thiosemicarbazone), 1742 ($\nu_{C=O}$ ester), 1677 ($\nu_{C=O}$ lactone), 1721 ($\nu_{C=O}$ lactone), 1614 ($\nu_{C=N}$), 1557 ($\nu_{C=C}$ arene), 1366 ($\nu_{C=S}$), 1229 and 1065 (ν_{COC} ester); ^{1}H NMR (500 MHz, DMSO-d_6), δ (ppm): 11.08 (s, 1H, H-b), 8.76 (d, J = 6.5 Hz, 1H, H-a), 8.26 (s, 1H, H-4′), 7.71 (d, J = 7.0 Hz, 1H, H-5′), 7.67 (t, J = 7.0 Hz, 1H, H-6′), 7.54 (t, J = 7.5 Hz, 1H, H-7′), 7.48 (d, J = 7.5 Hz, 1H, H-8′), 5.58−5.57 (m, Hz, 1H, H-1), 5.33–5.32 (m, 1H, H-4), 5.25–5.24 (m, 1H, H-3), 4.98–4.96 (m, 1H, H-2), 4.20–4.19 (m, 2H, H-6a and H-6b), 4.04–4.02 (m, 1H, H-5), 2.39 (s, 3H, C=N–CH_3), 2.01–1.94 (s, 4 × 3H, 4 × CH_3CO ester); ^{13}C NMR (125 MHz, DMSO-d_6), δ (ppm): 178.21, 171.03, 170.05, 169.73, 169.45, 155.15, 151.45, 150.44, 135.73, 132.76, 127.90, 125.31, 118.36, 117.12, 116.50, 79.53, 71.82, 70.96, 69.62, 67.18, 62.06, 20.82, 20.80, 20.71, 20.66, 14.83; ESI-HRMS(+): $C_{26}H_{29}N_3O_{11}S$, calcd. for M + H = 592.1601 Da, M + Na = 614.1420 Da, found: *m/z* 592.1607 ($[M+H]^+$), 614.1428 ($[M+Na]^+$).

3-Acetyl-6-chlorocoumarin *N*-(2,3,4,6-tetra-*O*-acetyl-β-D-galactopyranosyl)thiosemicarbazone (5b)

From **3b** (1 mmol, 445 mg) and 4 (1 mmol, 421 mg). Microwave irradiation time: 30 min. Yield: 325 mg (52%) of **5b** as yellow crystals from 96% ethanol. M.p.: 160−161 °C; $[\alpha]_D^{25}$ +78.1 (*c* 0.24, $CHCl_3$). 3313 (ν_{NH}), 1738 ($\nu_{C=O}$ ester), 1623 ($\nu_{C=O}$ lactone), 1610 ($\nu_{C=N}$), 1520 and 1490 ($\nu_{C=C}$ arene), 1371 ($\nu_{C=S}$), 1230 and 1051 (ν_{COC} ester); ^{1}H NMR (500 MHz, DMSO-d_6), δ (ppm): ^{1}H NMR (500 MHz, DMSO-d_6), δ (ppm): 11.08 (s, 1H, H-b), 8.76 (d, J = 6.5 Hz, 1H, H-a), 8.26 (s, 1H, H-4′), 7.97 (d, J = 1.0 Hz, 1H, H-5′), 7.58 (t, J = 8.5 Hz, 1H, H-7′), 7.48 (d, J = 8.5 Hz, 1H, H-8′), 5.58−5.57 (m, Hz, 1H, H-1), 5.33−5.32 (m, 1H, H-4), 5.25−5.24 (m, 1H, H-3), 4.97−4.96 (m, 1H, H-2), 4.20–4.19 (m, 2H, H-6a and H-6b), 4.04–4.01 (m, 1H, H-5), 2.38 (s, 3H, C=N-CH_3), 2.01–1.94 (s, 4 × 3H, 4 × CH_3CO ester); ^{13}C NMR (125 MHz, DMSO-d_6), δ (ppm): 178.88, 171.02, 169.73, 169.33, 169.04, 158.60, 151.52, 149.45, 135.15, 132.90, 130.31, 128.28, 118.94, 118.45, 118.40, 79.87, 72.09, 70.33, 70.03, 66.44, 62.84, 21.24, 21.14, 20.71, 20.59, 14.99; EI-HRMS(+): $C_{26}H_{28}{}^{35}ClN_3O_{11}S$/ $C_{26}H_{28}{}^{37}ClN_3O_{11}S$, 625.1133/627.1104 Da, calcd. for M+H = 626.1211/628.1182 Da, found: *m/z* 626.1217/628.1189 ($[M+H]^+$).

3-Acetyl-6-bromocoumarin *N*-(2,3,4,6-tetra-*O*-acetyl-β-D-galactopyranosyl)thiosemicarbazone (5c)

From **3c** (1 mmol, 267 mg) and 4 (1 mmol, 421 mg). Microwave irradiation time: 30 min. Yield: 390 mg (58%)

of **5c** as yellow crystals from 96% ethanol. M.p.: 159–160 °C; $[\alpha]_D^{25}$ +79.3 (*c* 0.25, $CHCl_3$). IR (KBr), ν (cm^{-1}): 3447 and 3316 (ν_{NH}), 1730 ($\nu_{C=O}$ ester), 1671 ($\nu_{C=O}$ lactone), 1607 ($\nu_{C=N}$), 1524 ($\nu_{C=C}$ arene), 1370 ($\nu_{C=S}$), 1230 and 1055 (ν_{COC}ester); ^{1}H NMR (500 MHz, DMSO-d_6), δ (ppm): 11.02 (s, 1H, H-b), 8.76 (d, J = 7.0 Hz, 1H, H-a), 8.20 (s, 1H, H-4′), 7.97 (d, J = 8.5 Hz, 1H, H-7′), 7.90 (s, 1H, H-5′), 7.18 (d, J = 8.5 Hz, 1H, H-8′), 5.58–5.57 (m, Hz, 1H, H-1), 5.33–5.32 (m, 1H, H-4), 5.25–5.24 (m, 1H, H-3), 4.97–4.96 (m, 1H, H-2), 4.20–4.19 (m, 2H, H-6a and H-6b), 4.04–4.01 (m, 1H, H-5), 2.36 (s, 3H, C=N–CH_3), 2.01−1.95 (s, 4 × 3H, 4 × CH_3CO ester); ^{13}C NMR (125 MHz, DMSO-d_6), δ (ppm): 178.24, 170.97, 170.05, 169.73, 169.45, 158.54, 151.53, 150.28, 135.38, 135.09, 130.49, 118.65, 118.25, 117.69, 117.16, 79.67, 71.97, 71.18, 69.62, 67.11, 62.48, 21.68, 20.66, 20.29, 20.02, 15.47; ESI-HRMS(+): $C_{26}H_{28}{}^{79}BrN_3O_{11}S$/$C_{26}H_{28}{}^{81}BrN_3O_{11}S$, calcd. for M+H = 670.0706/672.0686 Da, found: *m/z* 670.0715/672.0694 ($[M+H]^+$).

3-Acetyl-6-methylcoumarin *N*-(2,3,4,6-tetra-*O*-acetyl-β-D-galactopyranosyl)thiosemicarbazone (5d)

From **3d** (1 mmol, 202 mg) and 4 (1 mmol, 421 mg). Microwave irradiation time: 40 min. Yield: 345 mg (57%) of **5d** as yellow crystals from 96% ethanol. M.p.: 309 −310 °C; $[\alpha]_D^{25}$ +82.3 (*c* 0.25, $CHCl_3$). IR (KBr), ν (cm^{-1}): 3443 (ν_{NH}), 1734 ($\nu_{C=O}$ ester and $\nu_{C=O}$ lactone), 1618 ($\nu_{C=N}$), 1561 and 1478 ($\nu_{C=C}$ arene), 1374 ($\nu_{C=S}$), 1228 and 1058 (ν_{COC}ester); ^{1}H NMR (500 MHz, DMSO-d_6), δ (ppm): 11.11 (s, 1H, H-b), 8.76 (d, J = 6.5 Hz, 1H, H-a), 8.06 (s, 1H, H-4′), 7.50 (s, 1H, H-5′), 7.19 (d, J = 8.25 Hz, 1H, H-8′), 7.14 (d, J = 8.25 Hz, 1H, H-7′), 5.58–5.57 (m, Hz, 1H, H-1), 5.33–5.32 (m, 1H, H-4), 5.25–5.24 (m, 1H, H-3), 4.97–4.96 (m, 1H, H-2), 4.20–4.19 (m, 2H, H-6a and H-6b), 4.04–4.02 (m, 1H, H-5), 2.38 (s, 3H, C=N–CH_3), 2.35 (s, 3H, 6-CH_3), 2.01 −1.95 (s, 4 × 3H, 4 × CH_3CO ester); ^{13}C NMR (125 MHz, DMSO-d_6), δ (ppm): 178.66, 171.66, 170.02, 169.73, 169.45, 158.50, 151.41, 148.72, 136.11, 135.55, 135.48, 129.54, 118.83, 116.93, 116.83, 79.40, 72.17, 71.05, 69.51, 67.11, 61.91, 20.96, 20.82, 20.79, 20.73, 20.65, 14.72; ESI-HRMS(+): $C_{27}H_{31}N_3O_{11}S$, calcd. for M+H = 606.1758 Da, M+Na = 628.1577 Da, found: *m/z* 606.1766 ($[M+H]^+$), 628.1584 ($[M+Na]^+$).

3-Acetyl-7-methylcoumarin *N*-(2,3,4,6-tetra-*O*-acetyl-β-D-galactopyranosyl)thiosemicarbazone (5e)

From **3e** (1 mmol, 202 mg) and 4 (1 mmol, 421 mg). Microwave irradiation time: 40 min. Yield: 240 mg (40%) of **5e** as yellow crystals from 96% ethanol. M.p.: 194–195 °C; $[\alpha]_D^{25}$ +80.3 (c = 0.26, $CHCl_3$). IR (KBr), ν (cm^{-1}): 3441 (ν_{NH}), 1736 ($\nu_{C=O}$ ester & $\nu_{C=O}$ lactone), 1616 ($\nu_{C=N}$), 1521 and 1470 ($\nu_{C=C}$ arene), 1371 ($\nu_{C=S}$), 1227 and 1057 (ν_{COC}ester); ^{1}H NMR (500 MHz, DMSO-d_6), δ (ppm): 11.14 (s, 1H, H-b), 8.77 (d, J = 6.5 Hz, 1H, H-a), 8.25 (s, 1H, H-4′), 7.50 (s, 1H, H-5′), 7.48 (d, J = 8.75 Hz, 1H, H-5′), 7.09 (d, J = 8.75 Hz, 1H, H-6′), 7.01 (s, 1H, H-8′), 5.58−5.57 (m, Hz, 1H, H-1), 5.33–5.32 (m, 1H, H-4), 5.25–5.24 (m, 1H, H-3), 4.97–4.95 (m, 1H, H-2), 4.20–4.19 (m, 2H, H-6a and H-6b), 4.05–4.01 (m, 1H, H-5), 2.38 (s, 3H, C=N–CH_3), 2.33 (s, 3H, 7-CH_3), 2.01–1.95 (s, 4 × 3H, 4 × CH_3CO ester); ^{13}C NMR (125 MHz, DMSO-d_6), δ (ppm): 178.64, 171.33, 170.05, 169.73, 169.45, 161.34, 151.51, 151.45, 136.50, 135.72, 128.23, 125.79, 118.32, 116.74, 113.74, 80.20, 72.13, 70.96, 68.54, 67.18, 61.41, 21.50, 21.13, 20.82, 20.71, 20.66, 15.00.; ESI-HRMS(+): $C_{27}H_{31}N_3O_{11}S$, calcd. for M+H = 606.1758 Da, M+Na = 628.1577 Da, found: *m/z* 606.1767 ($[M+H]^+$), 628.1584 ($[M+Na]^+$).

3-Acetyl-8-methoxycoumarin *N*-(2,3,4,6-tetra-*O*-acetyl-β-D-galactopyranosyl)thiosemicarbazone (5f)

From **3f** (1 mmol, 218 mg) and 4 (1 mmol, 421 mg). Microwave irradiation time: 35 min. Yield: 285 mg (46%) of **5f** as yellow crystals from 96% ethanol. M.p.: 217–218 °C; $[\alpha]_D^{25}$ +81.4 (*c* 0.24 $CHCl_3$). IR (KBr), ν (cm^{-1}): 3348 and 3220 (ν_{NH}), 1764 ($\nu_{C=O}$ ester), 1729 ($\nu_{C=O}$ lactone), 1610 ($\nu_{C=N}$), 1570 and 1523 ($\nu_{C=C}$ arene), 1371 ($\nu_{C=S}$), 1234 and 1042 (ν_{COC} ester); ^{1}H NMR (500 MHz, DMSO-d_6), δ (ppm): 11.11 (s, 1H, H-b), 8.76 (d, J = 7.0 Hz, 1H, H-a), 8.09 (s, 1H, H-4′), 7.46 (d, J = 8.5 Hz, 1H, H-5′), 7.23 (t, J = 8.25 Hz, 1H, H-6′), 7.10 (d, J = 8.25 Hz, 1H, H-7′), 5.59–5.56 (m, Hz, 1H, H-1), 5.34–5.31 (m, 1H, H-4), 5.26–5.24 (m, 1H, H-3), 4.98–4.95 (m, 1H, H-2), 4.20–4.19 (m, 2H, H-6a and H-6b), 4.04–4.01 (m, 1H, H-5), 3.92 (s, 3H, 8-OCH_3), 2.38 (s, 3H, C=N–CH_3), 2.01–1.94 (s, 4 × 3H, 4 × CH_3CO ester); ^{13}C NMR (125 MHz, DMSO-d_6), δ (ppm): 178.50, 171.04, 170.08, 169.73, 169.45, 161.70, 151.44, 147.48, 141.89, 133.13, 126.68, 122.65, 118.94, 117.55, 115.33, 80.20, 72.70, 70.96, 69.62, 67.18, 62.06, 56.10, 21.61, 21.24, 20.82, 20.71, 14.24; ESI-HRMS(+): $C_{27}H_{31}N_3O_{12}S$, calcd. for M+H = 622.1707 Da, M+Na = 644.1526 Da, found: *m/z* 622.1716 ($[M+H]^+$), 644.1531 ($[M+Na]^+$).

3-Acetyl-4-methylcoumarin *N*-(2,3,4,6-tetra-*O*-acetyl-β-D-galactopyranosyl)thiosemicarbazone (5g)

From **3g** (1 mmol, 202 mg) and 4 (1 mmol, 421 mg). Microwave irradiation time: 40 min. Yield: 205 mg (34%) of **5g** as yellow crystals from 96% ethanol. M.p.:

203–204 °C; $[\alpha]_D^{25}$ +80.3 (*c* 0.23, $CHCl_3$). IR (KBr), ν (cm^{-1}): 3443 (ν_{NH}), 1737 ($\nu_{C=O}$ ester and $\nu_{C=O}$ lactone), 1617 ($\nu_{C=N}$), 1521 and 1470 ($\nu_{C=C}$ arene), 1371 ($\nu_{C=S}$), 1227 and 1057 (ν_{COC}ester); ^{1}H NMR (500 MHz, DMSO-d_6), δ (ppm): 11.24 (s, 1H, H-b), 8.76 (d, J = 7.0 Hz, 1H, H-a), 7.76 (d, J = 8.0 Hz, 1H, H-5′), 7.57 (t, J = 8.0 Hz, 1H, H-7′), 7.41 (d, J = 8.0 Hz, 1H, H-8′), 7.25 (t, J = 8.0 Hz, 1H, H-6′), 5.59–5.56 (m, Hz, 1H, H-1), 5.34–5.31 (m, 1H, H-4), 5.27–5.24 (m, 1H, H-3), 4.98–4.95 (m, 1H, H-2), 4.20–4.19 (m, 2H, H-6a and H-6b), 4.05–4.02 (m, 1H, H-5), 2.94 (s, 3H, 4-CH_3), 2.35 (C=N–CH_3), 2.01–1.94 (s, 4 × 3H, 4 × CH_3CO ester); ^{13}C NMR (125 MHz, DMSO-d_6), δ (ppm): 178.97, 171.03, 170.48, 169.73, 169.02, 160.73, 153.85, 150.74, 143.94, 133.38, 124.26, 124.17, 118.97, 117.58, 114.39, 80.31, 72.10, 71.60, 68.45, 67.18, 61.43, 21.65, 20.92, 20.69, 19.96, 17.08, 16.79; ESI-HRMS(+): $C_{27}H_{31}N_3O_{11}S$, calcd. for M+H = 606.1758 Da, M+Na = 628.1577 Da, found: *m/z* 606.1767 ([M+H]$^+$), 628.1585 ([M+Na]$^+$).

3-Acetyl-7-hydroxy-4-methylcoumarin *N*-(2,3,4,6-tetra-*O*-acetyl-β-D-galactopyranosyl)thiosemicarbazone (5h)

From **3h** (1 mmol, 218 mg) and 4 (1 mmol, 421 mg). Microwave irradiation time: 40 min. Yield: 315 mg (51%) of **5h** as yellow crystals from 96% ethanol. M.p.: 153 −154 °C; $[\alpha]_D^{25}$ +82.2 (*c* 0.25, $CHCl_3$). IR (KBr), ν (cm^{-1}): 3354 and 3328 (ν_{NH}), 1751 ($\nu_{C=O}$ ester and $\nu_{C=O}$ lactone), 1616 ($\nu_{C=N}$), 1522 and 1495 ($\nu_{C=C}$ arene), 1372 ($\nu_{C=S}$), 1224 and 1062 (ν_{COC}ester); ^{1}H NMR (500 MHz, DMSO-d_6), δ (ppm): 11.24 (s, 1H, H-b), 10.93 (s, 1H, 7-OH), 8.76 (d, J = 7.0 Hz, 1H, H-a), 7.63 (d, J = 8.5 Hz, 1H, H-5′), 6.83 (d, J = 8.5 Hz, 1H, H-6′), 6.82 (s, 1H, H-8′), 5.58–5.57 (m, Hz, 1H, H-1), 5.33–5.32 (m, 1H, H-4), 5.27–5.25 (m, 1H, H-3), 4.97–4.96 (m, 1H, H-2), 4.20–4.19 (m, 2H, H-6a and H-6b), 4.05–4.02 (m, 1H, H-5), 3.92 (s, 3H, 8-OCH_3), 2.83 (s, 3H, 4-CH_3), 2.35 (C=N–CH_3), 2.01–1.94 (s, 4 × 3H, 4 × CH_3CO ester); ^{13}C NMR (125 MHz, DMSO-d_6), δ (ppm): 178.27, 171.12, 170.26, 169.73, 169.26, 161.58, 160.62, 153.78, 152.49, 143.99, 125.71, 114.15, 113.16, 112.93, 102.63, 79.55, 71.90, 70.58, 69.62, 67.04, 61.83, 21.91, 20.82, 20.71, 20.45, 17.08, 16.9; ESI-HRMS(+): $C_{27}H_{31}N_3O_{12}S$ M, calcd. for M+H = 622.1707 Da, M+Na = 644.1526 Da, found: *m/z* 622.1713 ([M+H]$^+$), 644.1531 ([M+Na]$^+$).

3-Acetyl-4-hydroxycoumarin *N*-(2,3,4,6-tetra-*O*-acetyl-β-D-galactopyranosyl)thiosemicarbazone (5i)

From **3i** (1 mmol, 204 mg) and 4 (1 mmol, 421 mg). Microwave irradiation time: 35 min. Yield: 460 mg (76%) of **5i** as yellow crystals from 96% ethanol. M.p.: 171 −172 °C; $[\alpha]_D^{25}$ +79.8 (*c* 0.23, $CHCl_3$). IR (KBr), ν (cm^{-1}): 3384 (ν_{NH}), 1723 ($\nu_{C=O}$ ester), 1648 ($\nu_{C=O}$ lactone), 1603 ($\nu_{C=N}$), 1552 ($\nu_{C=C}$ arene), 1327 ($\nu_{C=S}$), 1240 and 1098 (ν_{COC} ester); ^{1}H NMR (500 MHz, DMSO-d_6), δ (ppm): 14.48 (s, 1H, 4-OH), 11.36 (s, 1H, H-b), 8.76 (d, J = 7.5 Hz, 1H, H-a), 7.91 (d, J = 8.0 Hz, 1H, H-5′), 7.50 (t, J = 8.0 Hz, 1H, H-7′), 7.28 (d, J = 8.0 Hz, 1H, H-8′), 7.20 (t, J = 8.0 Hz, 1H, H-6′), 5.59–5.56 (m, Hz, 1H, H-1), 5.34–5.31 (m, 1H, H-4), 5.27–5.24 (m, 1H, H-3), 4.98 −4.95 (m, 1H, H-2), 4.20–4.19 (m, 2H, H-6a and H-6b), 4.04–4.01 (m, 1H, H-5), 2.28 (C=N–CH_3), 2.01–1.94 (s, 4 × 3H, 4×CH_3CO ester); ^{13}C NMR (125 MHz, DMSO-d_6), δ (ppm): 178.19, 171.03, 170.05, 169.73, 169.45, 166.88, 161.36, 155.74, 152.50, 132.86, 124.65, 124.10, 116.39, 112.50, 103.10, 80.72, 73.80, 70.64, 69.03, 68.73, 62.00, 20.92, 20.80, 20.71, 20.59, 17.12; ESI-HRMS(+): $C_{27}H_{31}N_3O_{12}S$, calcd. for M+H = 608.1550 Da, M+Na = 630.1370 Da, found: *m/z* 608.1555 ([M+H]$^+$), 630.1376 ([M+Na]$^+$).

3-Acetyl-4-hydroxy-8-methylcoumarin *N*-(2,3,4,6-tetra-*O*-acetyl-β-D-galactopyranosyl)thiosemicarbazone (5j)

From **3j** (1 mmol, 218 mg) and 4 (1 mmol, 421 mg). Microwave irradiation time: 30 min. Yield: 405 mg (65%) of **5j** as yellow crystals from 96% ethanol. M.p.: 161 −162 °C; $[\alpha]_D^{25}$ +78.9 (*c* 0.23, $CHCl_3$). IR (KBr), ν (cm^{-1}): 3499 and 3234 (ν_{NH}), 1748 ($\nu_{C=O}$ ester and $\nu_{C=O}$ lactone), 1606 ($\nu_{C=N}$), 1574, 1500 and 1486 ($\nu_{C=C}$ arene), 1373 ($\nu_{C=S}$), 1225 and 1050 (ν_{COC} ester); ^{1}H NMR (500 MHz, DMSO-d_6), δ (ppm): 14.28 (s, 1H, 4-OH), 11.36 (s, 1H, H-b), 8.76 (d, J = 6.5 Hz, 1H, H-a), 7.84 (d, J = 8.0 Hz, 1H, H-5′), 7.32 (d, J = 8.0 Hz, 1H, H-7′), 7.09 (t, J = 8.0 Hz, 1H, H-6′), 5.59–5.57 (m, Hz, 1H, H-1), 5.33–5.32 (m, 1H, H-4), 5.25–5.24 (m, 1H, H-3), 4.98–4.95 (m, 1H, H-2), 4.20–4.19 (m, 2H, H-6a and H-6b), 4.04–4.01 (m, 1H, H-5), 2.32 (s, 3H, 8-CH_3), 2.28 (C=N–CH_3), 2.01–1.94 (s, 4 × 3H, 4 × CH_3CO ester); ^{13}C NMR (125 MHz, DMSO-d_6), δ (ppm): 178.43, 171.22, 170.05, 169.73, 169.45, 166.25, 160.67, 155.70, 151.42, 133.20, 127.84, 124.67, 121.39, 110.52, 105.96, 79.07, 73.16, 70.98, 69.62, 67.50, 62.71, 21.34, 20.82, 20.71, 19.72, 17.85, 17.04; ESI-HRMS (+): $C_{27}H_{31}N_3O_{12}S$, calcd. for M+H = 622.1707 Da, M +Na = 644.1526 Da, found: *m/z* 622.1714 ([M+H]$^+$), 644.1531 ([M+Na]$^+$).

Biological assays

In vitro cytotoxic assay

Dilution series (128, 32, 16, 8, 4, 2, 1, and 0.5 µg/mL of each compound 5a-5j) were prepared and used for MTT assay [33]. Two cancer cell lines were seeded at a density of 3 × 10^4 cells/well and treated with a range of concentrations in triplicate in

96-well cell culture plates, whereupon cell proliferation was assessed using a standard MTT assay. Specifically, the growth inhibitory activity of benzothiazepines was determined using MTT, which correlates the cell number with the mitochondrial reduction of MTT to a blue formazan precipitate. In brief, the cells were plated in 96-well plates and allowed to attach overnight. The medium was then replaced with serum-free medium containing the test compounds and cells were incubated at 37 °C for 72 h. The medium was then replaced with a fresh medium containing 1 mg/mL MTT. Following incubation at 37 °C for 2–4 h, the wells were aspirated, the dye was solubilized in DMSO and the absorbance was measured at 540 nm using a Tecan™ GENios® Microplate Reader (Conquer Scientific, USA). The viability of cells was compared with that of the control cells. The slope of the absorbance change was used for calculating the reaction rate. Negative controls were performed in the absence of enzyme and compound, and positive controls in the presence of enzyme and 100% DMSO. The percentage of residual activity was calculated as the difference in absorbance between the time 6 and 2 min, obtained by the average of two experiments carried out in triplicate. The obtained rate was related to the rate when the inhibitor was absent. IC_{50} values were calculated from linear extrapolations of reaction rate (as a function of the logarithm of the concentration). The IC_{50} values were determined with increasing concentrations of inhibitor versus % of inhibition, in triplicate in two independent experiments. The experiment was done in triplicate and the IC_{50} values were obtained through non-linear regression using the software GraphPad Prism version 7.0.

EGFR inhibition assay and annexin-V assay

EGFR inhibition assay was performed on HepG2 cells using cloud clone SEA757Hu 96 Kit, following the same instructions from the manufacturer protocol through homogeneous time-resolved fluorescence assay. The fraction of the EGFR was measured in the presence of the tested compounds using the equation: $E_{(\%)} = E_{max}/(1 + [I]/ID_{50})$, E_{max} is the activity in the absence of the inhibitor, [I] is the inhibitor concentration and ID_{50} is the inhibitor concentration when $E_{(\%)} = 0.5\ E_{max}$, then the dose-response curve was plotted. Inhibitory activity against EGFR L858R-TK and EGFR T790M-TK was performed using HTRF (homogeneous time-resolved fluorescence) assay method [44]. Different kinases and ATP were obtained from Sigma. The specified kinase and its substrate were incubated with tested compounds /reference drug for 5 min in buffer solution to start the enzymatic reaction, ATP was then added to the reaction mixture and maintained for 30 min at room temperature. Stopping the reaction was performed by adding detection reagents containing EDTA for 1 h then the IC_{50} values were determined by GraphPad Prism version 7.0.

Annexin-V assay

HepG2 cells were seeded in a 96-well plate (1×10^5 cells/well), incubated for 24 h, then treated with vehicle (0.1% DMSO) or 10 mM of tested compounds, **5a** and **5b**, for 24 h. The cells were then harvested, washed using PBS, and stained for 15 min at room temperature in the dark using annexin V-FITC and PI in binding buffer (10 mM HEPES, 140 mM NaCl and 2.5 mM $CaCl_2$ at pH 7.4), then analyzed by the flow cytometer [45].

Molecular docking

The two-dimensional structures (.mae) of selected compounds (ligands) **5a**, **5b**, **5c**, and **5h**, and Erlotinib were drawn and the structure was analyzed by using a 2D sketcher and 3D builder of Maestro version 12.5 (Schrödinger suite 2020-3) [37] according to a previous method [46]. The three-dimensional structures of these compounds (ligands) were generated from three-dimensional structures prepared by conformational search tool using OPLS-2005 force field for geometrically minimizing with MacroModel version 12.9 followed by conformational analysis using MMFFs force field. Monte Carlo Multiple Minimum (MCMM) conformational search was used with 2500 iterations and a convergence threshold of 0.05 kJ/mol. Water was chosen as solvent. Truncated Newton Conjugate Gradient minimization was used with 2500 iterations and a convergence threshold of 0.05 kJ/mol. Other parameters were used as default.

Crystallographic structure of EGFR tyrosine kinase domain with Erlotinib was retrieved from Protein Data Bank (PDB ID: 4HJO, resolution 2.75 Å, https://www.rcsb.org/structure/4HJO) and considered as a target for docking simulations. Coordinates of the protein-ligand complex were fixed for errors in atomic representations and optimized using Protein Preparation Wizard Maestro version 11.5 (Maestro, v. 11.5: Schrödinger, LLC, New York, NY, USA). The bond orders were assigned to residues, hydrogen atoms were added at pH 7.0 ± 2.0. The restrained minimizations were carried out using the OPLS 2005 force field with an RMSD cut-off value of 0.3 Å for heavy atom convergences. The molecular docking was accomplished and analyzed via the Glide version 8.8 docking tool. The receptor grid was located in the center based on the active site of the protein, using the receptor grid generation tool. The Glide HTVS 8.8 algorithm (High-Throughput Virtual Screening Mode) was employed using a grid box volume of $10 \times 10 \times 10$ Å. Briefly, Glide approximates a systematic search of positions, orientations, and conformations of the ligand in the receptor-binding site using a series of hierarchical filters. The bond orders were assigned to residues, hydrogen

atoms were added at pH 7.0 ± 2.0. The restrained minimizations were carried out using the OPLS 2005 force field with an RMSD cut-off value of 0.3 Å for heavy atom convergences.

Compliance with ethical standards

Conflict of interest The authors declare no competing interests.

Publisher's note Springer Nature remains neutral with regard to jurisdictional claims in published maps and institutional affiliations.

References

1. Stefanachi A, Leonetti F, Pisani L, Catto M, Carotti A. Coumarin: a natural, privileged and versatile scaffold for bioactive compounds. Molecules. 2018;23:250 https://doi.org/10.3390/molecules23020250.
2. Annunziata F, Pinna C, Dallavalle S, Tamborini L, Pinto A. An overview of coumarin as a versatile and readily accessible scaffold with broad-ranging biological activities. Int J Mol Sci. 2020;21:4618 https://doi.org/10.3390/ijms21134618.
3. Khan MS, Agrawal R, Ubaidullah M, Hassan MI, Tarannum N. Design, synthesis and validation of anti-microbial coumarin derivatives: an efficient green approach. Heliyon. 2019;5:e02615 https://doi.org/10.1016/j.heliyon.2019.e02615.
4. Alshibl HM, Al-Abdullah ES, Haiba ME, Alkahtani HM, Awad GEA, Mahmoud AH, et al. Synthesis and evaluation of new coumarin derivatives as antioxidant, antimicrobial, and anti-inflammatory agents. Molecules. 2020;25:3251 https://doi.org/10.3390/molecules25143251.
5. Narayan B, Anupa AK, Yuba Raj P, Paras Nath Y. Anticancer potential of coumarin and its derivatives. Mini-Rev Med Chem. 2021;21:1–1. https://doi.org/10.2174/1389557521666210405160323.
6. Ranjan Sahoo C, Sahoo J, Mahapatra M, Lenka D, Kumar Sahu P, Dehury B, et al. Coumarin derivatives as promising antibacterial agent(s). Arab J Chem. 2021;14:102922 https://doi.org/10.1016/j.arabjc.2020.102922.
7. Al-Warhi T, Sabt A, Elkaeed EB, Eldehna WM. Recent advancements of coumarin-based anticancer agents: an up-to-date review. Bioorg Chem. 2020;103:104163 https://doi.org/10.1016/j.bioorg.2020.104163.
8. Kasmi R, Hadaji E, Chedadi O, El Aissouq A, Bouachrine M, Ouammou A. 2D-QSAR and docking study of a series of coumarin derivatives as inhibitors of CDK (anticancer activity) with an application of the molecular docking method. Heliyon. 2020;6:e04514 https://doi.org/10.1016/j.heliyon.2020.e04514.
9. Maleki EH, Bahrami AR, Sadeghian H, Matin MM. Discovering the structure–activity relationships of different O-prenylated coumarin derivatives as effective anticancer agents in human cervical cancer cells. Toxicol Vitr. 2020;63:104745 https://doi.org/10.1016/j.tiv.2019.104745.
10. Goel R, Luxami V, Paul K. Synthesis, in vitro anticancer activity and SAR studies of arylated imidazo[1,2-*a*]pyrazine–coumarin hybrids. RSC Adv. 2015;5:37887–95. https://doi.org/10.1039/C5RA00584A.
11. Carotti A, Carrieri A, Chimichi S, Boccalini M, Cosimelli B, Gnerre C, et al. Natural and synthetic geiparvarins are strong and selective MAO-B inhibitors. synthesis and SAR studies. Bioorg Med Chem Lett. 2002;12:3551–55. https://doi.org/10.1016/S0960-894X(02)00798-9.
12. Jain M, Kapadia R, Jadeja RN, Thounaojam MC, Devkar RV, Mishra SH. Hepatoprotective activity of Feronia limonia root. J Pharm Pharm. 2012;64:888–96. https://doi.org/10.1111/j.2042-7158.2012.01481.x.
13. Govindaiah P, Dumala N, Mattan I, Grover P, Jaya Prakash M. Design, synthesis, biological and in silico evaluation of coumarin-hydrazone derivatives as tubulin targeted antiproliferative agents. Bioorg Chem. 2019;91:103143 https://doi.org/10.1016/j.bioorg.2019.103143.
14. Elshemy HAH, Zaki MA. Design and synthesis of new coumarin hybrids and insight into their mode of antiproliferative action. Bioorg Med Chem. 2017;25:1066–75. https://doi.org/10.1016/j.bmc.2016.12.019.
15. Goud NS, Kanth Makani VK, Pranay J, Alvala R, Qureshi IA, Kumar P, et al. Synthesis, ^{18}F-radiolabeling and apoptosis inducing studies of novel 4, 7-disubstituted coumarins. Bioorg Chem. 2020;97:103663 https://doi.org/10.1016/j.bioorg.2020.103663.
16. Bonaccorso C, Grasso G, Musso N, Barresi V, Condorelli DF, La Mendola D, et al. Water soluble glucose derivative of thiocarbohydrazone acts as ionophore with cytotoxic effects on tumor cells. J Inorg Biochem. 2018;182:92–102. https://doi.org/10.1016/j.jinorgbio.2018.01.019.
17. Vekariya RH, Patel KD, Rajani DP, Rajani SD, Patel HD. A one pot, three component synthesis of coumarin hybrid thiosemicarbazone derivatives and their antimicrobial evolution. J Assoc Arab Univ Basic Appl Sci. 2017;23:10–19. https://doi.org/10.1016/j.jaubas.2016.04.002.
18. Yang G, Jin Q, Xu C, Fan S, Wang C, Xie P. Synthesis, characterization and antifungal activity of coumarin-functionalized chitosan derivatives. Int J Biol Macromol. 2018;106:179–84. https://doi.org/10.1016/j.ijbiomac.2017.08.009.
19. Naasani N, Harbal J, Kandil F. Synthesis and biological evaluation of 3-thiosemicarbazoneacetyl coumarin derivatives as antioxidant. Res J Pharm Technol. 2020;13:4565–69. https://doi.org/10.5958/0974-360X.2020.00804.5.
20. Kalaiarasi G, Rex Jeya Rajkumar S, Aswini G, Dharani S, Fronczek FR, Prabhakaran R. 3-Acetyl-8-methoxy-2[H]-chromen-2-one derived Schiff bases as potent antiproliferative agents: insight into the influence of 4(N)-substituents on the in vitro biological activity. Spectrochim Acta A. 2018;200:246–62. https://doi.org/10.1016/j.saa.2018.04.028.
21. Varma M, Shravage B, Tayade S, Kumbhar A, Butcher R, Jani V, et al. A simple methyl substitution of 3-acetylcoumarin thiosemicarbazone enhances cellular autophagy flux, reduces inflammation and ameliorates rough eye phenotype in the Drosophila model of Alzheimer's disease. J Mol Struct. 2021;1235:130265 https://doi.org/10.1016/j.molstruc.2021.130265.
22. Fonseca NC, da Cruz LF, da Silva Villela F, do Nascimento Pereira GA, de Siqueira-Neto JL, Kellar D, et al. Synthesis of a sugar-based Thiosemicarbazone series and structure-activity relationship versus the parasite cysteine proteases Rhodesain, Cruzain, and *Schistosoma mansoni* Cathepsin B1. Antimicrob Agents Chemother. 2015;59:2666–77. https://doi.org/10.1128/aac.04601-14.
23. Thanh ND, Giang NTK, Quyen TH, Huong DT, Toan VN. Synthesis and evaluation of in vivo antioxidant, in vitro antibacterial, MRSA and antifungal activity of novel substituted isatin *N*-(2,3,4,6-tetra-*O*-acetyl-β-D-glucopyranosyl)thiosemicarbazones. Eur J Med Chem. 2016;123:532–43. https://doi.org/10.1016/j.ejmech.2016.07.074.
24. Wang X, Goldstein D, Crowe PJ, Yang J-L. Next-generation EGFR/HER tyrosine kinase inhibitors for the treatment of patients with non-small-cell lung cancer harboring EGFR mutations: a review of the evidence. OncoTargets Ther. 2016;9:5461–73. https://doi.org/10.2147/OTT.S94745.

25. Schneider MR, Wolf E. The epidermal growth factor receptor ligands at a glance. 2009;218:460–66. https://doi.org/10.1002/jcp.21635.
26. Barbuti AM, Zhang G-N, Gupta P, Narayanan S, Chen Z-S. Chapter 1—EGFR and HER2 inhibitors as sensitizing agents for cancer chemotherapy. In: Chen Z-S, Yang D-H, editors. Protein kinase inhibitors as sensitizing agents for chemotherapy. 1st. ed.: Academic Press; 2019. pp. 1–11.
27. Howe LR, Brown PH. Targeting the HER/EGFR/ErbB family to prevent breast cancer. Cancer Prev Res. 2011;4:1149–57. https://doi.org/10.1158/1940-6207.CAPR-11-0334.
28. Sueangoen N, Tantiwetrueangdet A, Panvichian R. HCC-derived EGFR mutants are functioning, EGF-dependent, and erlotinib-resistant. Cell Biosci. 2020;10:41 https://doi.org/10.1186/s13578-020-00407-1.
29. Stadlbauers W, Hojas G. Ring closure reactions of 3-arylhydrazonoalkyl-quinolin-2-ones to 1-aryl-pyrazolo[4,3-c]quinolin-2-ones. J Heterocycl Chem. 2004;41:681–90. https://doi.org/10.1002/jhet.5570410505.
30. Gao W-T, Hou W-D, Zheng M-R, Tang L-J. Clean and convenient one-pot synthesis of 4-hydroxycoumarin and 4-hydroxy-2-quinolinone derivatives. Synth Commun. 2010;40:732–38. https://doi.org/10.1080/00397910903013713.
31. Park SJ, Lee JC, Lee KI. A facile synthesis of 4-hydroxycoumarin and 4-hydroxy-2-quinolone derivatives. Bull Korean Chem Soc. 2007;28:1203–05. https://doi.org/10.5012/bkcs.2007.28.7.1203.
32. Russell A, Frye JR. 2,6-Dihydroxyacetophenone. Organic syntheses. Organic Syntheses, Inc.; 2003. 22-22.
33. Scudiero DA, Shoemaker RH, Paull KD, Monks A, Tierney S, Nofziger TH, et al. Evaluation of a soluble tetrazolium/formazan assay for cell growth and drug sensitivity in culture using human and other tumor cell lines. Cancer Res. 1988;48:4827–33. https://cancerres.aacrjournals.org/content/canres/48/17/4827.full.pdf https://cancerres.aacrjournals.org/content/canres/48/17/4827.full.pdf.
34. Abdelbaset MS, Abdel-Aziz M, Ramadan M, Abdelrahman MH, Abbas Bukhari SN, Ali TFS, et al. Discovery of novel thienoquinoline-2-carboxamide chalcone derivatives as anti-proliferative EGFR tyrosine kinase inhibitors. Bioorg Med Chem. 2019;27:1076–86. https://doi.org/10.1016/j.bmc.2019.02.012.
35. Park Jin H, Liu Y, Lemmon Mark A, Radhakrishnan R. Erlotinib binds both inactive and active conformations of the EGFR tyrosine kinase domain. Biochem J. 2012;448:417–23. https://doi.org/10.1042/BJ20121513.
36. Liang Y, Zhang T, Zhang J. Natural tyrosine kinase inhibitors acting on the epidermal growth factor receptor: Their relevance for cancer therapy. Pharm Res. 2020;161:105164 https://doi.org/10.1016/j.phrs.2020.105164.
37. Schrödinger. Release 2020-3. New York, NY (USA): Schrödinger, Inc.; 2020. http://www.schrodinger.com.
38. Hirai T, Togo H. Preparation and synthetic use of polymer-supported acetoacetate reagent. Synthesis. 2005;2005:2664–68. https://doi.org/10.1055/s-2005-872142.
39. Czerney P, Hartmann H. Einfache darstellung von *N*-(2′-hydroxy)-aryliden-nitro-anilinen als cumarin-synthone. J Prakt Chem. 1982;324:21–28. https://doi.org/10.1002/prac.19823240105.
40. Dean FM, Robertson A, Whalley WB. The chemistry of fungi. Part IX. 3: 4-dihydrocoumarins. J Chem Soc. 1950;182:895–902. https://doi.org/10.1039/JR9500000895.
41. Liu X-H, Fan J-C, Liu Y, Shang Z-C. L-Proline as an efficient and reusable promoter for the synthesis of coumarins in ionic liquid. J Zhejiang Univ Sci B. 2008;9:990–95. https://doi.org/10.1631/jzus.B0820079.
42. Ramani A, Chanda MB, Velu S, Sivasanker S. One-pot synthesis of coumarins. Catalysis by the solid base, calcined Mg-Al hydrotalcite. Green Chem. 1999;1:163–65. https://doi.org/10.1039/A903173A.
43. Venkateswara Rao K, Sundaramurthy V. A convenient one-step synthesis of 3-acetyl-4-hydroxycoumarins. Proc Indian Acad Sci Sect A. 1975;81:118–23. https://doi.org/10.1007/BF03051136.
44. Jia Y, Quinn CM, Gagnon AI, Talanian R. Homogeneous time-resolved fluorescence and its applications for kinase assays in drug discovery. Anal Biochem. 2006;356:273–81. https://doi.org/10.1016/j.ab.2006.05.006.
45. Lo KK-W, Lee TK-M, Lau JS-Y, Poon W-L, Cheng S-H. Luminescent biological probes derived from ruthenium(II) estradiol polypyridine complexes. Inorg Chem. 2008;47:200–08. https://doi.org/10.1021/ic701735q.
46. Toan DN, Thanh ND, Truong MX, Van DT. Quinoline-pyrimidine hybrid compounds from 3-acetyl-4-hydroxy-1-methylquinolin-2(1*H*)-one: study on synthesis, cytotoxicity, ADMET and molecular docking. Arab J Chem. 2020;13:7860–74. https://doi.org/10.1016/j.arabjc.2020.09.018.